CHAPTER 4

MICROWAVE HEATING OF CONCRETES AND REINFORCED CONCRETE

4.1 Introduction

This chapter presents the microwave-assisted heating of concrete materials and reinforced concrete, *i.e.*, cement pastes containing pozzolan materials, mortars, and concretes are explored in detail here both experimentally and numerically. The first section experimentally investigates the interaction between microwave energy and Type I cement–based materials with and without pozzolan materials during the first 24 hours hydration period. The second section investigates the microstructural characteristics of hydration products in cement-based materials subjected to microwave-irradiated energy based on constant microwave-power levels, and compares the results for the same kinds of materials subjected to conventional and high-temperature curing methods. The next chapter will propose a microstructural development for concrete materials' pastes subjected to high-temperature curing using microwave energy.

4.2 Extended scope of the research

o The mix proportions of cement-based materials include water-to-solid (Type I Portland cement with/without pozzolan materials; water-to-solid ratios (w/s) (0.25 (compatible with stoichiometry and consisting of anhydrous cement), 0.38 (fully hydrated paste) and 0.45 (hydration product and capillary pores)). The chemical admixture uses a superplasticizer agent that conforms to the ASTM C 494 Type F (polycarboxylate-based admixture): that is, the superplasticizer agent has a recommended dosage rate of 1000 ml per 100 kg of total solid materials content, which is the replacement level of a pozzolan material; the agent also has pulverized fuel ash (FA), metakaolinite (MK), and silica fume (SF) as 20 %wt. of its solid materials content.

o The surrounding parameters at the water-to-solid ratio (w/s) of 0.38 include pressure levels at normal pressure (760 ± 5 mm Hg, torr).

o The properties of Type I Portland cement are its composition (X-ray Fluorescence (XRF)) and physical properties (particle size distribution (particle size analyzer)) and surface morphology (Scanning electron microscopy (SEM)).

- Conditions of curing
  - Saturated lime water (temperature: 25 ± 2 ^{0}C)
  - Microwave energy: constant power levels
    - Delay time of 30 minutes, initial setting time, and final setting time
    - Power levels: 50 ± 5, 100 ± 5 and 150 ± 5 watt
    - Times of application: 0, 10, 20 and 30 minutes
- Properties of cement-based materials
  - Macroscopic: strength (axial load compression) at 8 hours, 24 hours, 7 days and 28 days, heat of hydration and temperature rise
  - Microscopic: surface morphology and compositions characteristic of C-S-H, $Ca(OH)_2$ and ettringite (X-ray diffraction), surface morphology and compositions (SEM-EDX), and thermogravimetric analysis (TGA-DTA)
- Microwave-heating model of cement paste: Heat-generation (conduction mode) model.

4.3 Materials and methods

4.3.1 Materials used

The starting materials used in this study included several commercial cementitious materials, i.e., Portland cement Type I, pulverized fuel ash (FA), metakaolin (MK), and condensed silica fume (SF). A variety of characterization techniques was used to determine the chemical composition and physical properties of these materials. Roll bar 12.0 mm diameter was used as reinforced steel embedded in cementtious materials.

4.3.1.1 Characterization of starting cementitious materials

The chemical composition of the Portland cement Type I OPC, FA, (CLASS F), MK, and condensed SF as weight percent was determined by means of a DC argon plasma spectrometer and trimetric analysis.

Deionized water with a pH value of 7.5 was used. Ottawa sand, which has a fineness modulus equal to 2.58, constitutes a fine aggregate accurately graded to pass a 850-μ (US Standard No. 20) sieve and to be retained on a 600-μ (US Standard No. 30) sieve—both of which are used to test cements. Crushed limestone rock with a fineness modulus and nominal maximum size equal to 5.75 and 5.90 cm respectively was used as coarse aggregate.

Moreover, the test results of specific gravity and absorption of aggregates are also listed in Table 3.2.

Chemical admixtures: Well-known commercially as Sikament 520 High Range Water Reducing Admixture, the superplasticizer conforms to the ASTM C 494, as comply with ASTM C 494 Type G. For general concrete applications, Sika recommends a dosage rate of between 500 – 1200 ml/100 kg) cementitious materials. If maximum water reduction is required, a dosage of 1400 ml/100 kg) of cementitious materials can be used. In this case, delayed setting times may occur.

4.3.2 Mixture proportions

The mixture proportioning was based on the above concepts. Table 4.1 shows the pastes, mortar, and concrete mixture. In addition, the water-to-solid mass ratio (w/s), pozzolan, aggregate mortar and concrete were studied. Tables 4.2 and 4.3 show the mixtures classified according to the curing method by which they are traditionally cured, i.e., conventional curing (Table 4.2) and rapid curing using microwave energy (Table 4.3). In particular, the group of mixtures that are typically cured using microwave energy, the water-to-solid mass ratio of 0.38 by weight was emphasized because it is well-known that this value consists entirely of hydration products.

Table 4.1 Mixtures used (by weight in grams).

Group	Factors affecting	Symbol	W/S	OPC (g)	FA (g)	SF (g)	MK (g)	Water (g)	Superplasticizer Type G (g)	Sand (g)	Rock (g)
1	Water-to-solid ratio, w/s	1CW/S_P0.25	0.25	500	0	0	0	125	0	0	0
		1CW/S_P0.38	0.38	500	0	0	0	190	0	0	0
		1CW/S_P0.45	0.45	500	0	0	0	225	0	0	0
2	Pozzolan	2CAP_0.38FA20_Super_10%	0.38	400	100	0	0	190	5	0	0
		2CAP_0.38MK20_Super_10%	0.38	400	0	0	100	190	5	0	0
		2CAP_0.38SF20_Super_10%	0.38	400	0	100	0	190	5	0	0
3	Aggregate, Mortar	3CAM0.38_1:2.75	0.38	500	0	0	0	0	5	1375	0
	Aggregate, Concrete	3CAC0.38_1:1:1	0.38	500	0	0	0	0	5	500	500

Table 4.2 Mixtures used (by weight in grams) with conventional curing.

Group	Factors affecting	Symbol	W/S	OPC (g)	FA (g)	SF (g)	MK (g)	Water (g)	Superplasticizer Type G (g)	Sand (g)	Rock (g)
1	(Saturated lime-deionized water)	1CW/S_P0.25	0.25	500	0	0	0	125	0	0	0
		1CW/S_P0.38	0.38	500	0	0	0	190	0	0	0
		1CW/S_P0.45	0.45	500	0	0	0	225	0	0	0
		2CAP_0.38FA20_Super_10%	0.38	400	100	0	0	190	5	0	0
		2CAP_0.38MK20_Super_10%	0.38	400	0	0	100	190	5	0	0
		2CAP_0.38SF20_Super_10%	0.38	400	0	100	0	190	5	0	0
		3CAM0.38_1:2.75	0.38	500	0	0	0	0	5	1375	0
		3CAC0.38_1:1:1	0.38	500	0	0	0	0	5	500	500

Table 4.3 Mixtures used (by weight in grams) with microwave energy.

Group	Factors affecting	Symbol	W/S	OPC (g)	FA (g)	SF (g)	MK (g)	Water (g)	Superplasticizer Type G (g)	Sand (g)	Rock (g)
1	Dormant period	1DP_50(30 min, initial set, final set)	0.38	500	0	0	0	190	0	0	0
		1DP_100(30 min, initial set, final set)	0.38	500	0	0	0	190	0	0	0
		1DP_150(30 min, initial set, final set)	0.38	500	0	0	0	190	0	0	0
2	Accelerated period	2AP_50 (10,20,30)	0.38	500	0	0	0	190	0	0	0
		2AP_100(10,20,30)	0.38	500	0	0	0	190	0	0	0
		2AP_150(10,20,30)	0.38	500	0	0	0	190	0	0	0
3	Sequential, Power level (time of application)	50(10)100(10)50(10)	0.38	500	0	0	0	190	0	0	0
		150(10)100(10)50(10)	0.38	500	0	0	0	190	0	0	0
		100(20)50(10)	0.38	500	0	0	0	190	0	0	0
		50(10)100(10)150(10)	0.38	500	0	0	0	190	0	0	0
		100(10)150(10)50(10)	0.38	500	0	0	0	190	0	0	0
		100(10)150(10)100(10)	0.38	500	0	0	0	190	0	0	0
		50(10)150(10)50(10)	0.38	500	0	0	0	190	0	0	0

4.3.3 Mixing and molding

The appropriate amounts of starting materials (Table 4.1) were weighed out to the nearest hundredth of a gram on a Mettler PI 1200 balance. A Hobart mixer was used to mix the solids and liquids according to ASTM C 109 (ASTM, 2009). Samples were cast 109.22 mm long, 54.61 mm wide, and 50 mm thick specimens for paste, mortar, and concrete. The samples were cured by using saturated lime water at 25 ^{0}C, microwave energy with a multimode cavity, or autoclaving.

The setting time was measured in accordance with ASTM C 191. Pastes were cast normally, and their compressive strengths were determined using 109.20 mm long, 54.60 mm wide, and 50 mm thick cube specimens. As well as, cement paste specimens, mortar specimens: Ottawa sand ratio was 1 : 2.75. The water-to-solid ratio was 0.38. For concrete, the cementitious materials: Ottawa sand: crushed limestone rock was 1:1:1. The water-to-solid ratio was 0.38. The specimens were removed from the mold 23½ ± ½ hours after the start of mixing and then cured by conventional curing, rapid curing with microwave energy, and rapid curing: autoclave curing. The specimens subjected to conventional curing were immersed in a $Ca(OH)_2$ saturated solution.

4.3.4 Microwave curing setup

For accelerated curing, the microwave system used was a monochromatic microwave at a frequency of 2.45 GHz, as shown in Fig. 4.1. Microwave energy was generated by a magnetron and transmitted directly along the propagation direction (+z) of a rectangular wave guide toward a water load situated at the end of the waveguide to ensure that a minimal amount of microwave energy would be reflected back to the sample. A warming water load was circulated through the cooling tower in order to reduce the temperature in the water load system.

A cement paste sample was arranged perpendicular to the propagation direction. A Type K thermo-couple with a 0.1 mm diameter was inserted at the center of the sample for the purpose of monitoring the temperature rise. During a 10-minutes period of microwave heating, the output of the microwave magnetron was controlled at 50, 100 and 150 W. The microwave plane wave traveled directly along the wave guide and made contact with the sample surface; the wave was then reflected and transmitted. By using a wattmeter, incident, reflected and transmitted waves were monitored.

For the specimens subjected to microwave curing, the delay times at 30 minutes after mixing, at the initial setting time, and at the final setting time are determined by the present

study for microwave application at the following power levels and durations: power levels of 50, 100, and 150 watt and times of 0, 10, 20, and 30 minutes. Furthermore, the decelerated period used normal cooling and vacuum conditions.

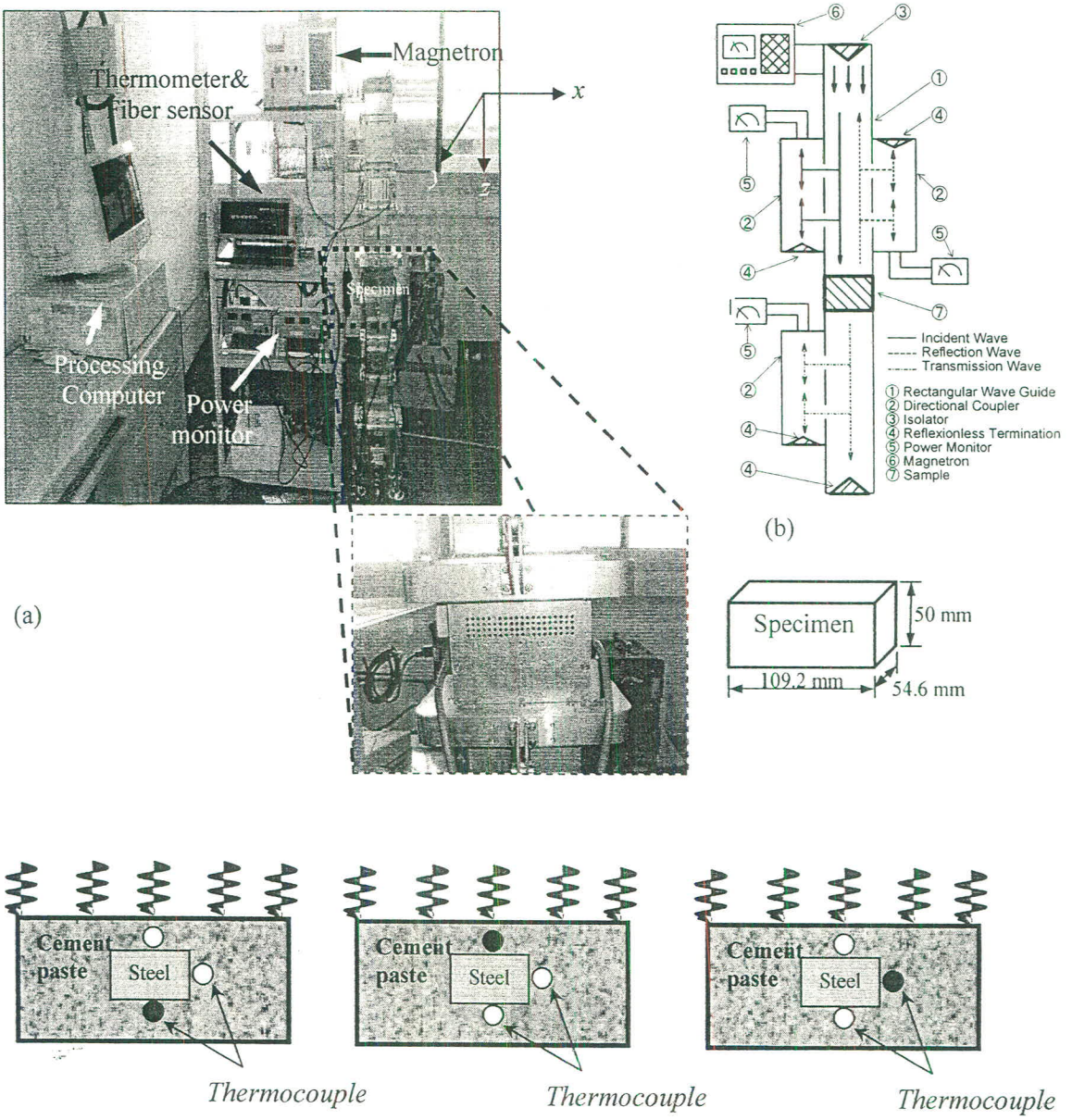

Fig. 4.1 (a) Experimental set up and (b) schematic showing direction of microwave components (Incident wave, reflected wave, and transmission wave), and (c), (d), (e) are the positions of thermocouples.

4.3.5 Equipment and procedures

4.3.5.1 Scanning Electron Microscope (SEM)

A Scanning Electron Microscope (SEM), specifically an International Scientific Instruments ISI-130 electron microscope, was used to determine the microstructure and morphology of the samples. A dual-stage, dual-screen microscope, it had five lenses and used an energy x-ray (EDX) analysis system. The maximum practical resolution was approximately 100,000 times. The specimens were glued onto a sample stub using carbon tape and then placed in a vacuum chamber and sputtered with gold for approximately 40 minutes at a 75 voltage. The gold film created a route by which the electrons could be conducted off the surface of the sample; otherwise, the accumulation of electrons on the sample surface would have led to charging and a fuzzy picture. The image was displayed on two 30 cm cathode ray tubes.

4.3.5.2 Microscopes: Powder X-ray Diffraction (XRD)

The crystalline phase identification of the various samples was performed on a Scintag X-ray Diffractometer. This differactometer is equipped with a copper target x-ray source, monochromator, and Tl-drifted NaI scintillation detector. Dried-powder samples were packed into a cavity of a zero-background quartz slide and placed on a goniometry. Most of the subsequent scans were taken from 0 to 70^0 2Θ at a rate of 2^0 2Θ per minute. The diffractometer is controlled by a VAX 3100 mini-computer and contains a matched software that can be used to display the data on the computer screen and through which data manipulation can be performed. The raw data can be downloaded into a personal computer and the results printed on either a Hewlett Packard plotter or a laser printer. This software package can distinguish between amorphous and crystalline peaks and between $K_{\alpha 1}$ and $K_{\alpha 12}$ peaks. In all cases, the raw data used contained some information pertaining to amorphous phases, in the form of humps in the spectra, which would otherwise have been stripped away by the software.

4.3.5.3 Thermal Analysis

Differential thermal analysis (DTA) of a few selected samples was conducted using a NETZSCH, STA449C Jupiter© analyzers (Sample temperature: 0.1 ^{o}C resolution, and better than 0.5 ^{o}C accuracy, Temperature range: room temperature to 1,550 ^{o}C and Heating rate: 0.1-99.9 ^{o}C /min). In all cases 40 – 50 mg of the sample were used, and alumina was the reference material. The heating rate was 10 ^{0}C/minutes, and the atmosphere was air. The

instrument was suitably adjusted in some cases to obtain the best thermograms in the temperature range of 30 to 600 ^{0}C.

4.3.5.4 Axial and unconfined load compressive strength

The respective compressive strengths of the cement pastes, mortars, and concrete samples were tested using a compressive strength apparatus in accordance with the ASTM C 39 at 8 hours, 24 hours, 3 days, and 28 days (Fig. 4.2).

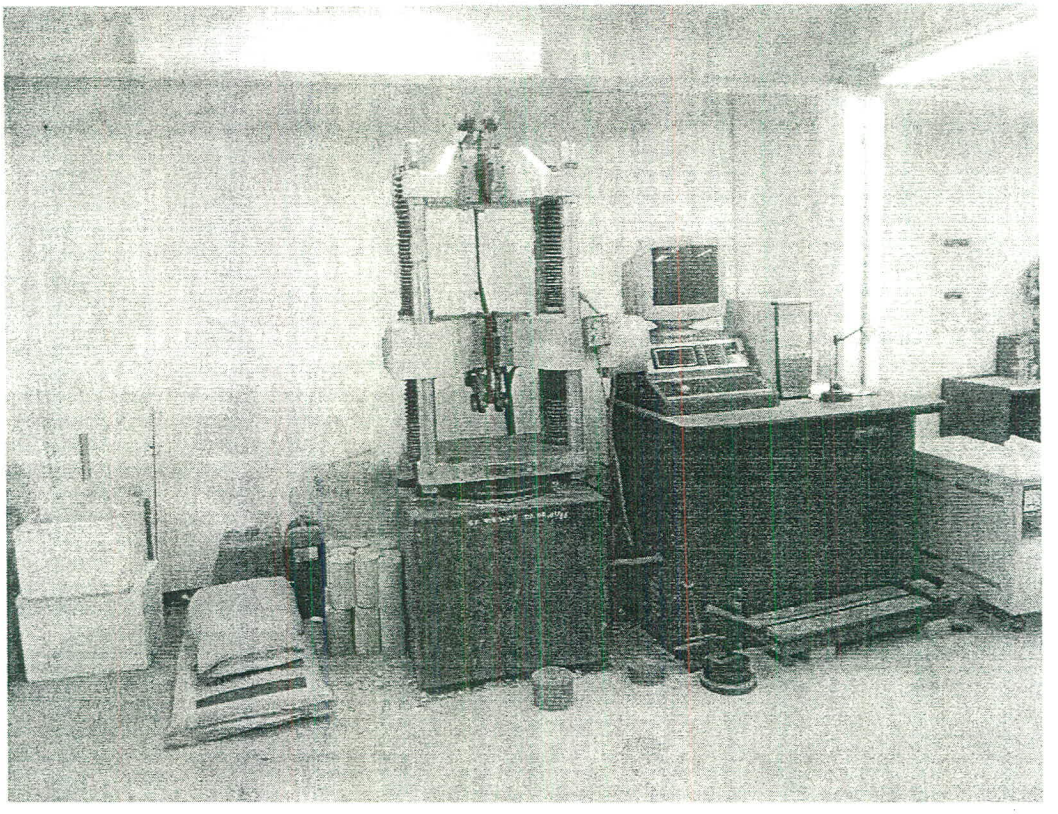

Fig. 4.2 Universal testing machine.

4.4 Results and discussion

4.4.1 Influence of the mix proportions of reinforced cementitious materials

4.4.2.1 Water-to-solid mass ratios (w/s)

The effect of water-to-solid ratios on microstructures characteristics of the reinforced pastes subjected microwave energy is presented. These characteristic is investigated by scanning electron microscope (SEM) with dispersive X-ray (EDX), X-ray diffraction (XRD) and thermal analysis (TG). The pastes used were proportioned at w/s ratios of 0.25, 0.38 and 0.45. After mixing and molding, they were cured at room temperature by wrapping with polyethylene plastic until the delay time (time after mixing until introducing microwave energy with a single-mode cavity) for 30 minutes The temperature profile and microwave power of 100 watt with a specific application time 30 minutes of the pastes is shown in Fig. 4.3. With limitation of the microwave equipment used, it can only adjust manually the steps of microwave power level such as 50, 100, 150, 200 ,..., 3000 watt, therefore the optimal microwave levels with the aforementioned research should be set at 100 ± 5 watt.

Temperature profiles obtained from averaging the five monitored data at bottom surface (Fig. 4.3(a)), top surface (Fig. 4.3(b)) and at the middle (Fig. 4.3(c)). The temperatures increase monotonically among the positions of measurement during the microwave curing process and reach a maximum of 105 ^{0}C at the bottom surface of the cured cement paste. Significantly, the paste at lower water-to-cement ratio experiences high temperature rise, or 1CW/S_P0.25 > 1CW/S_P0.38 > 1CW/S_P0.45. This is because of two inclusive effects; (i) heat liberation from hydration reaction is increased as low content of water in the system, and (ii) heat from interaction between the microwave energy and internal water leading to superposition of them. In other words, the addition heat from microwave energy can change the kinetics of hydration in accordance with Arrhenius's law.

When comparison the obtained temperatures at three positions, the bottom of the cured specimen has highest temperature levels than those of other sides. It may be due to that fact that during temperature rise, the water at the top side of specimen may evaporate, so the temperature was dropping gradually, while at the bottom the evaporation of water is difficult. As a result the heat accumulates on the specific side providing temperature increase with high rate than the other sides.

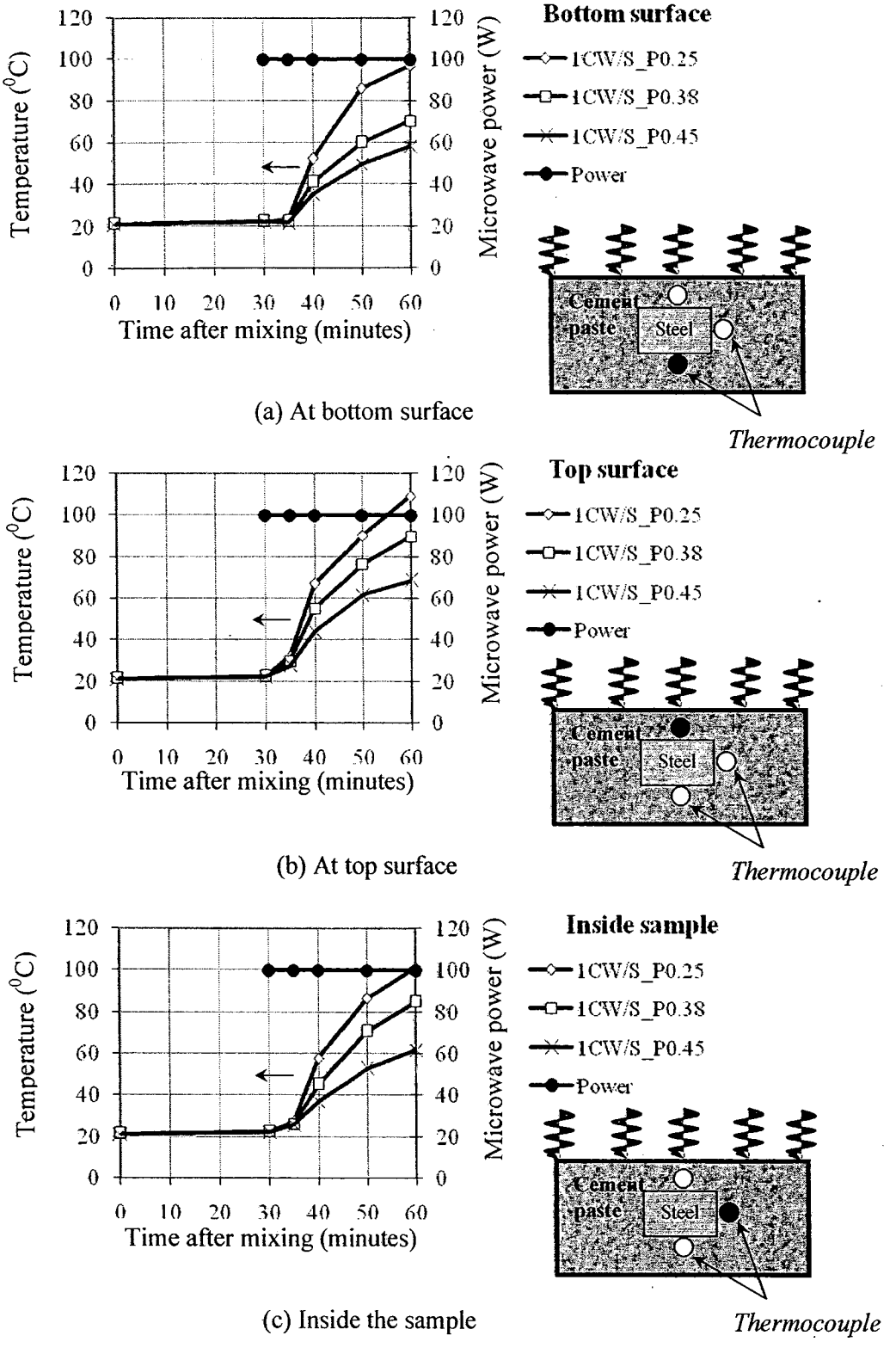

Fig. 4.3 Temperature and power history during applying microwave energy of various cement pastes with different water-to-solid mass ratios.

The typical micrographs of the 1CW/S_P0.38 paste at the age of 4 hours after mixing, 28 days after curing in lime-saturated deionized water, and subjected to microwave energy are shown in Fig. 4.4. It is clearly seen from Fig. 4.4(a) and 4.4(b) that the samples consist of hydrated phases and pores, as well as cores of $Ca(OH)_2$ dendrite crystals or other crystals (marked CH), calcium silicate hydrate (C-S-H), and granular structure. Furthermore, some ettringite (Aft) is found in case of specimens were cured by microwave energy. It can be described that in the early stages of reaction of the 27°C sample, very small (about 1 μm) irregularly-shaped ettringite was formed; but at the same curing time, needle-like ettringite had already formed in 60 °C samples.

(a) 1CW/S_P0.25 at the age of 4 hrs

(b) 1CW/S_P0.38 at the age of 4 hrs

(c) 1CW/S_P0.25 at the age of 28 days

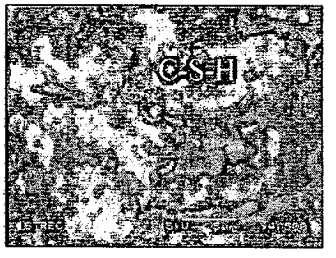

(d) 1CW/S_P0.38 at the age of 28 days

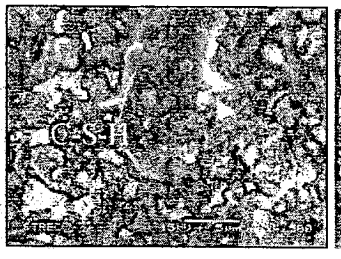

(e) 1CW/S_P0.25 after applying MW energy power 100 W for 30 min

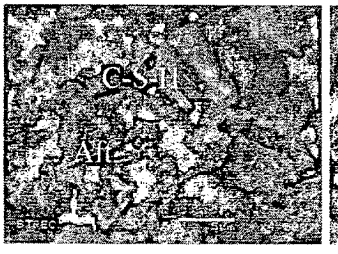

(f) 1CW/S_P0.38 applying MW energy power 100 W for 30 min

(g) 1CW/S_P0.45 applying MW energy power 100 W for 30 min

Fig. 4.4 Micrographs of various cement pastes with different water-to-solid ratios at 4 hours subjected to lime-saturated deionized water curing and microwave energy.

The composition of the calcium silicate hydrate (C-S-H) gel and other products formed in hydrated Portland cement systems has been studied in terms of its Ca/Si and Al/Ca ratios by several researchers [125,126] The results reported vary due to the individual characteristics of the cements hydrated and the conditions of hydration, as well as the experimental technique used for the characterization. Calculated Ca/Si ratios also can be obtained from the measured CH concentration and the degree of hydration of the calcium silicates. Cement hydration products are commonly classified as two products. The former are those hydration products formed within the original cement grain boundaries, and the latter are those products formed in the space initially occupied by water. Such definitions are used in this work. In the products, the main cement hydration product is C-S-H gel, which is principally responsible for the properties of the hydrated cement.

Spectrums of various cement pastes with different water-to-cement ratios at 4 hours subjected to normal curing (lime-saturated deionized water) and microwave energy are shown in Fig. 4.5. However, the results in the form of atomic (molar) ratios of several elements with respect to calcium, from the EDS analysis composition are also represented Fig. 4.6. It shows plots of the Al/Ca ratio versus the Si/Ca ratio for the pastes hydrated at microwave power 390 watt for 45 minutes. The (X) corresponds to the 0.45-w/s paste analyses, as the hydration temperature decreases from 100° to 62°C, the Al/Ca ratio changes from 0.022 to 0.091, and Si/Ca ratio varies from 0.141 to 0.263.

From the SEM–EDS results it was observed, although the measured Ca/Si ratios of the pastes were similar in magnitude that they consistently decreased when the temperature was decreased from 100° to 62°C. In this study, the same SEM equipment was always used and an effort was made to perform all the analyses under essentially the same experimental conditions. Hence, the trends are believed to be reliable, even if the absolute values are not. Some results in the literature agree with this observed trend, but some others differ. Sorption of sulfate ions by C-S-H gel, as discussed below, may require extra calcium ions for charge balance, hence providing a mechanism for decreasing in this ratio. The observed decrease in the Ca/Si ratio was, however, small and similar in magnitude to the standard deviation of the results. In an independent investigation, the difference between the Ca/Si ratios, this ratio and its variation with curing temperature may vary with the extent of solid solution of foreign ions incorporated in the C-S-H gel and the amount of other phases, notably CH, intermixed in the gel phase. It seems prudent to conclude overall that, until analyses can be obtained with lower errors, the Ca/Si ratio does not vary in a systematic way with an increase in the curing

temperature. It also has been observed that, for the cement pastes cured at the highest temperature, more sulfur and less aluminum are retained in the pastes.

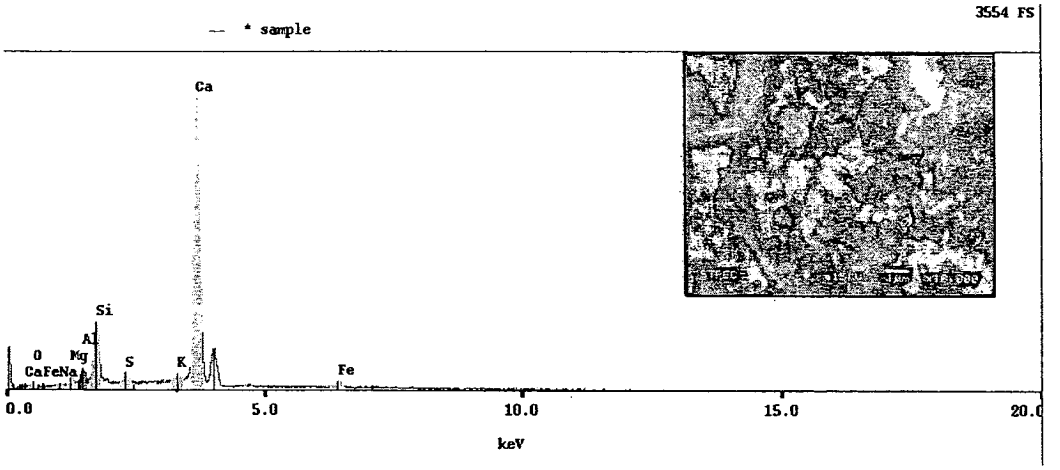

(a) 1CW/S_P0.25 after applying a microwave power 100 watt for 30 minutes

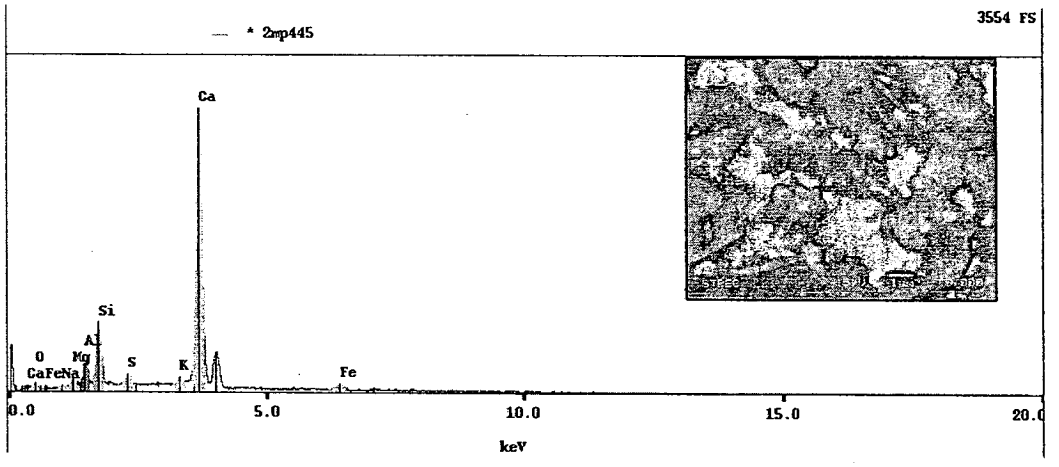

(b) 1CW/S_P0.38 after applying microwave power 100 watt for 30 minutes

Fig. 4.5 Spectrums of various cement pastes with different water-to-solid ratios at 4 hours subjected to normal curing (lime-saturated deionized water) and microwave energy.

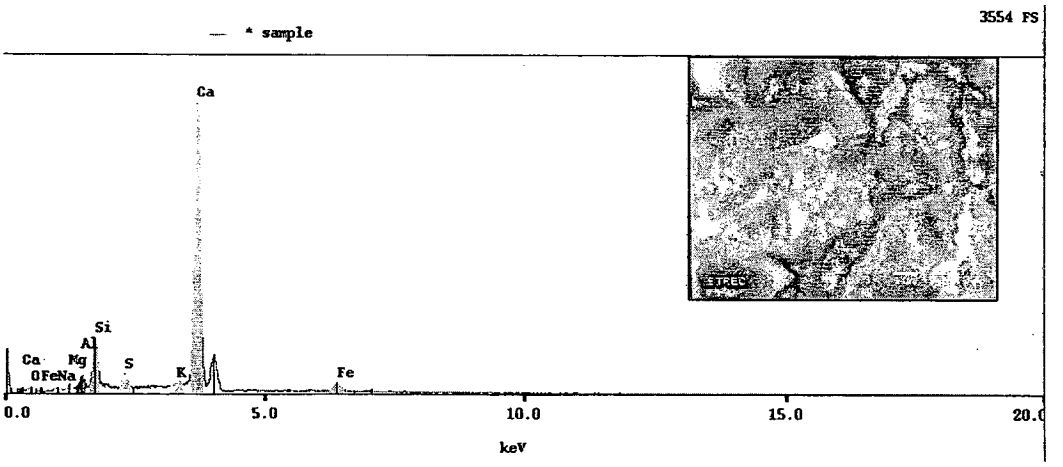

(c) 1CW/S_P0.45 after applying microwave power 100 watt for 30 minutes

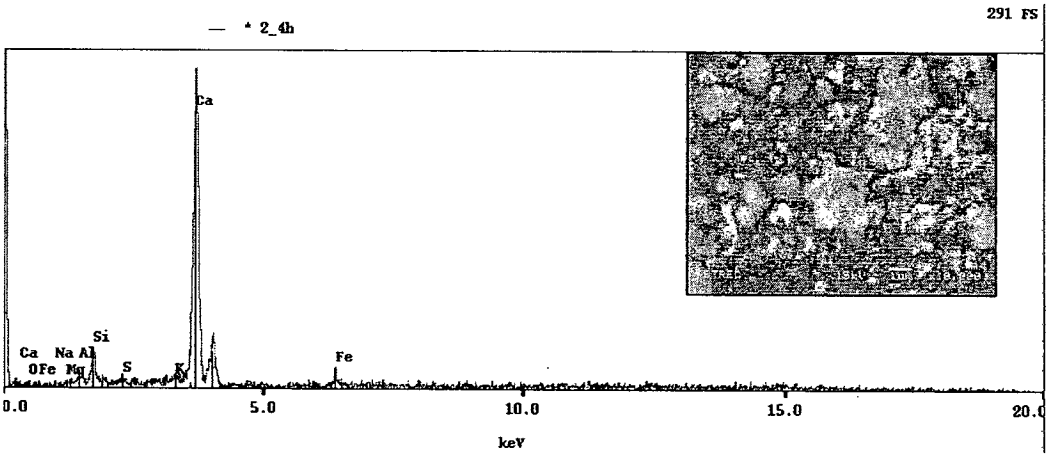

(d) 1CW/S_P0.38 at the age of 4 hours

Fig. 4.5 (Cont.) Spectrums of various cement pastes with different water-to-solid ratios at 4 hours subjected to normal curing (lime-saturated deionized water) and microwave energy.

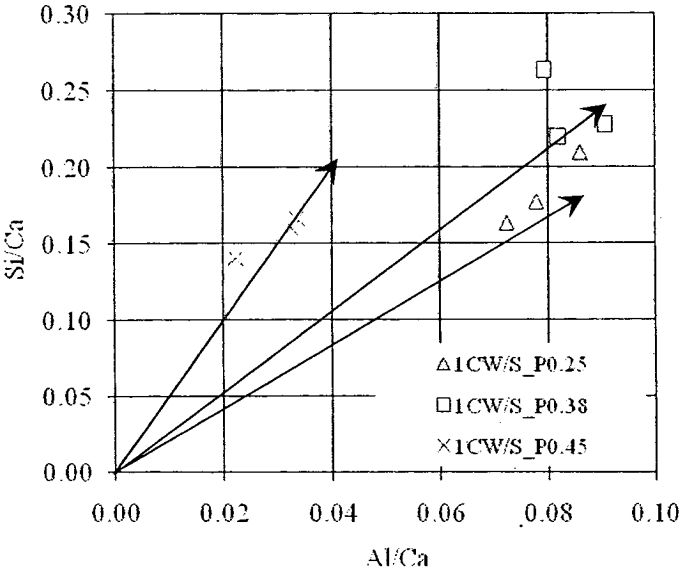

Fig. 4.6 Atom ratio of Si/Ca versus Al/Ca of the pastes of 1CW/S_P0.25, 1CW/S_P0.38 and 1CW/S_P0.45 after applying microwave energy power 100 watt for 30 minutes.

X-ray diffractometry was used to determine the degree of crystallinity of the hydrated cement products and the existence of crystalline coexisting phases. Fig. 4.7 shows x-ray patterns of the hydrated products in the pastes of 1CW/S_P0.38 after applying microwave power 100 watt for 30 minutes. The phases identified include calcium silicate hydrate (Ca_3SiO_5), calcium hydroxide ($Ca(OH)_2$), residual lime (CaO) and Xenotile ($Ca_6(SiO_3)_6(H_2O)$).

Regarding the effect of water-to-solid ratios on the phase characteristics of 1CW/S_P0.25, 1CW/S_P0.38 and 1CW/S_P0.45 after applying microwave power of 100 watt for 30 minutes as shown in Fig. 4.7, it is found that the calcium silicate hydrate (Ca_3SiO_5), calcium hydroxide ($Ca(OH)_2$) phases are similar.

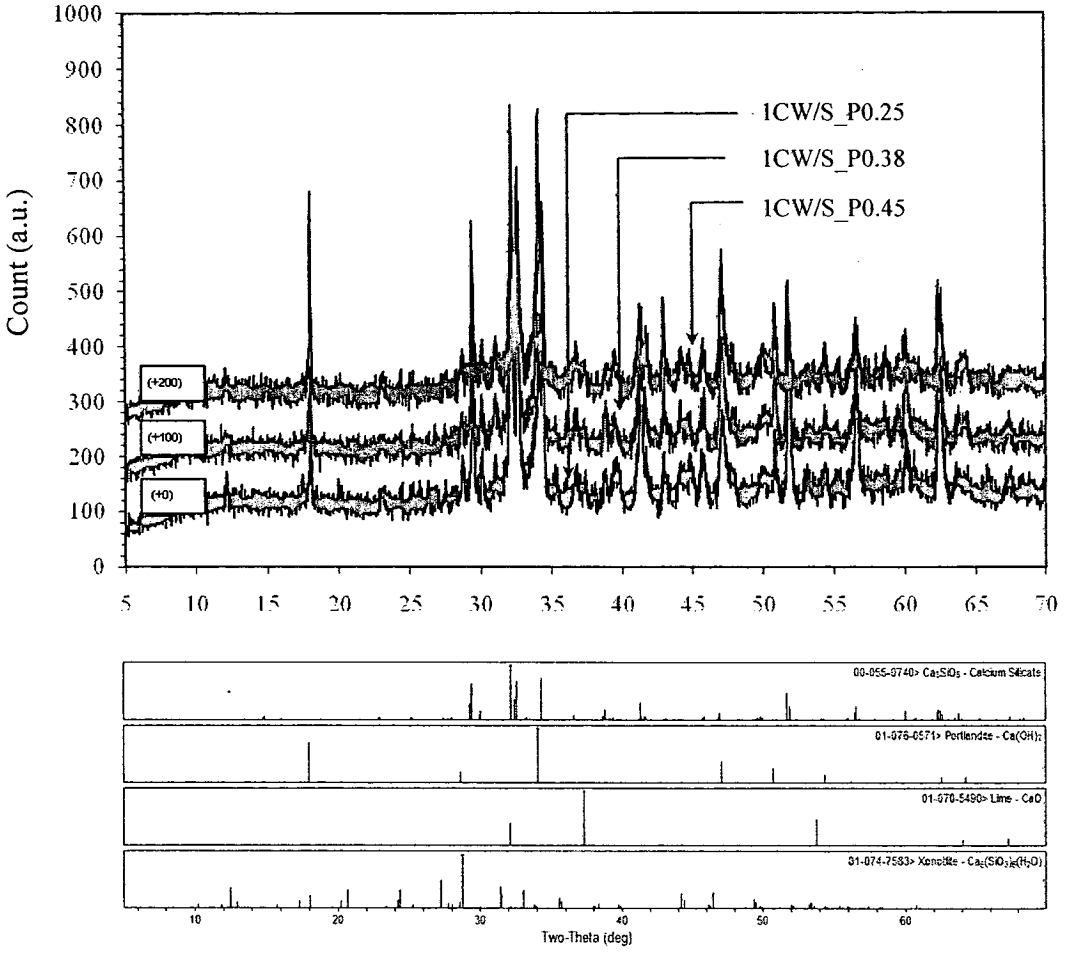

Fig. 4.7 X-ray diffraction of the pastes of 1CW/S_P0.25, 1CW/S_P0.38 and 1CW/S_P0.45 after applying MW power 100 watt for 30 minutes.

Compressive strengths of the pastes of 1CW/S_P0.25, 1CW/S_P0.38 and 1CW/S_P0.45 after applying microwave power of 390 watt for 45 minutes compared to normal curing are shown in Fig. 4.8. It was found that when cured at elevated temperatures, pastes develop strength quite rapidly. At the age of 8 hrs after microwave curing at 100 ^{0}C (at middle) 1CW/S_P0.25 paste attained a strength of 25.1 MPa (239 % higher than the normal-cured paste); at 24 hours curing the strength was 68.3 MPa, and 7 and 28 days the strength were 74.9 and 75.2 MPa, respectively. For the elevated temperature curing with 1CW/S_P0.38 and 1CW/S_P0.45 pastes, the strength obtained at 8 hrs was 10.9 MPa, exceeding the strength of the paste cured without microwave energy. However, at 24 hrs and later ages the strength of the pastes cured at elevated temperature was 23 to 46 % lower than that of the paste cured at room temperature. This is due to decrease of the water-to-cement ratio less than about 0.40 [26,76]. According to Taylor [126], when water-to-cement ratio

should equals to 0.40, all the water molecules exist as gel and combined water in C-S-H structure; that is, there is no capillary water in the case of full hydration taking place. However, some capillary pores should be preserved as a path, through which water molecules can come in and react with cement grains near the pores. Meanwhile, these pores could serve as a space for gel expansion. The existence of a few capillary pores might be favorable for the structure and strength of the hardened cement paste. The above statement is consistent with our experimental results; that is if w/s ratio is less than 0.40, it is difficult for the full hydration of cement and unfavorable for the strength of concrete.

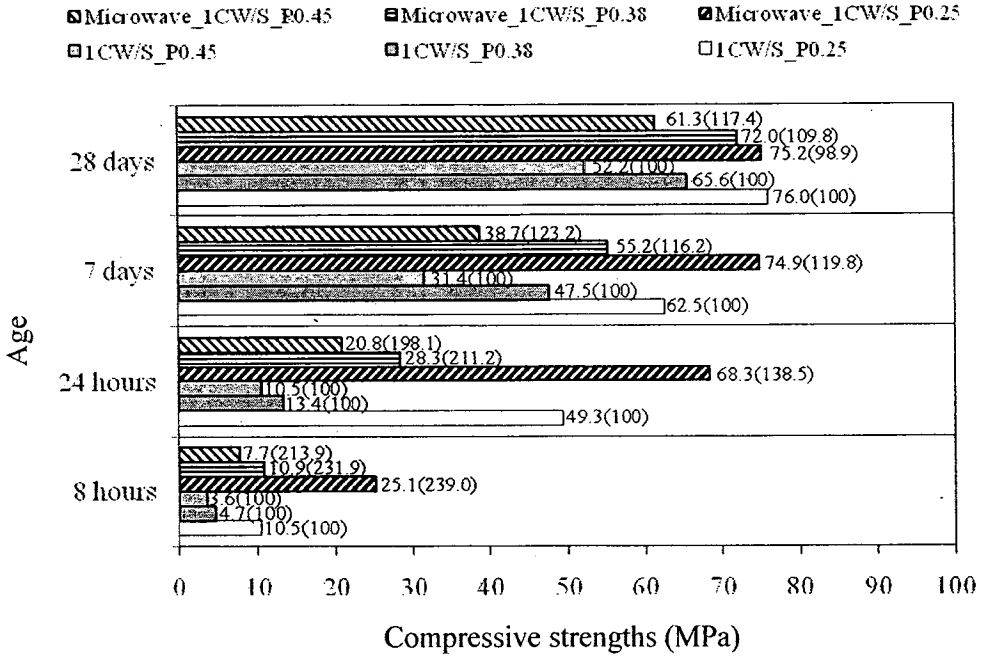

Fig. 4.8 Compressive strengths of the pastes of 1CW/S_P0.25, 1CW/S_P0.38 and 1CW/S_P0.45 after applying microwave power 390 watt for 45 minutes compared to normal curing.

The evaluation of the hydration rate in the microwave -cured and normal-cured cement pastes was based on the Thermogravimetry (TG) curves and consisted of the following steps: (a) determining the total combined water: this is the total water incorporated in the cement paste, which corresponds directly to weight loss of up to 550 ^{0}C; (b) determining the amount of $Ca(OH)_2$, which is found by weight loss in the range of 400–550 ^{0}C, converted to $Ca(OH)_2$, and then added to the carbonated $Ca(OH)_2$; and (c) determining the amount of water combined in the hydration products (other than calcium hydroxide), which corresponds directly to weight loss of up to 300 ^{0}C. Any changes in the water content of the

hydration products indicate that these compounds have changed in terms of how they are constituted and/or their stoichiometry.

Fig. 4.9 presents the weight loss that accrues from the water lost in the hydration reactions, the loss of $Ca(OH)_2$ content, and combined loss of water and $Ca(OH)_2$ content for the cement pastes when subjected to microwave energy of 390 watt for 45 minutes. It can be seen that the cement paste at w/s = 0.25, and that the total water, total $Ca(OH)_2$ content, and water and $Ca(OH)_2$ combined are 10.990%, 2.426%, and 4.514%, respectively. For the 0.38 paste, the corresponding figures are 10.998%, 2.723%, and 7.243%, respectively; for the 0.45 paste the figures are 13.889%, 2.587%, and 10.307% respectively. For $Ca(OH)_2$ content, the 0.38 w/s MW-cured paste is quite different from the others because this w/s is optimal for reacting to fully hydrated products, while the higher w/s pastes produce a low concentration of Ca^{2+} and OH^- and consequent to crystallize a low $Ca(OH)_2$ content (Taylor, 1997). Apart from $Ca(OH)_2$ content, for the case in which water was combined with Ca(OH), it is also similar to total water content in the hydration products.

In summary, when microwave power and time of application were kept, the relative water content of the pastes' hydration products were affected by different w/s, while their $Ca(OH)_2$ contents were affected due to the completion of hydration reaction which is occurred at the water-to-cement mass ratio (w/s) of 0.38 (Taylor, 1986), while a lower w/s is not sufficient ions (Ca^{2+} and OH^-) quantities, and a higher w/s is not concentration to crystalline.

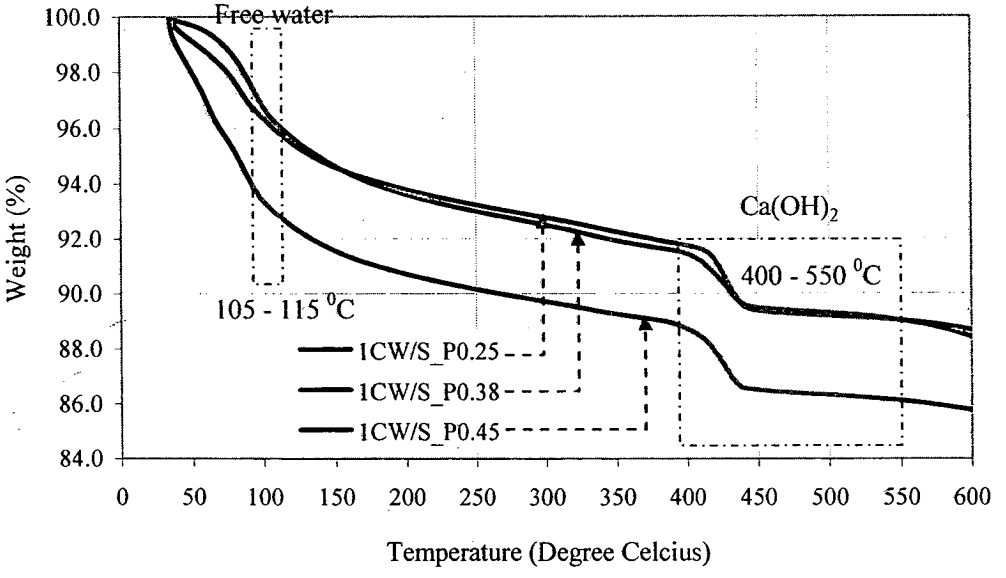

Fig. 4.9 Thermogravimetric analysis (TG) by comparison among different temperatures and weights.

4.4.2.2 Pozzolan materials in reinforced cement paste

The effects of microwave energy used with a multi-mode system on pozzolan materials are discussed in this section. Pulverized fuel ash (FA), matakaolin (MK), and silica fume (SF) were taken into account. The pastes containing pozzolan materials were proportioned at w/s ratios of 0.38 and were also replaced at 20 % by weight. After mixing and molding, they were wrapped in polyethylene plastic in order to be cured at room temperature with a delay time after mixing for 30 minutes. The temperature profile of the pastes at microwave power of 100 watt with a specific application time of 30 minutes is shown in Fig. 4.10. The temperature profiles were obtained by averaging the five monitored data at the top surface (Fig. 4.10(a)), at the bottom surface (Fig. 4.10(b)) and in the inside (Fig. 4.10(c)). The temperature increases monotonically among the points of measurement during the microwave-curing process and reached a maximum temperature of 89 ^{0}C at the bottom surface of the microwave-cured FA–cement paste, 72.9 ^{0}C at the bottom surface of the microwave-cured MK–cement paste, and 62.4 ^{0}C at the bottom surface of the microwave-cured SF–cement paste. Significantly, for pastes containing pozzolan temperature rise relates to the free water that remains the pozzolan has been absorbed, and the amount of heat that microwave energy generates is also decreased as well. It is well-known that the FA particles are more rounded in shape than are the MK and SF particles, and as a result the FA–cement paste shows the highest temperature increase of the three.

Furthermore, at early-age microwave curing, the rate at which the temperature increases is higher than the sequential temperature profile of the FA–cement paste increases. This is because the application of microwave energy accelerates rapidly the hydration [76] and pozzolan reactions and so affects the production of Portlandite ($Ca(OH)_2$). This is subsequent to an increase in the concentration of Portlandite, which, in turn, also speeds up the pozzolanic reaction. And, it should be noted that an increase in this reaction is accompanied by an increase in heat liberation or temperature rise.

Similar to the effects noted in the previous section, the bottom of the microwave-cured paste has higher temperature levels than do the top side or the inside. At the top side, the temperature level was affected by the rate at which the water evaporated of water; that is, the temperature dropped gradually; at the bottom water evaporation took place even more slowly. While the heat accumulated on the bottom side, and thus caused the temperature to increase more quickly at the bottom than at the other points of measurement.

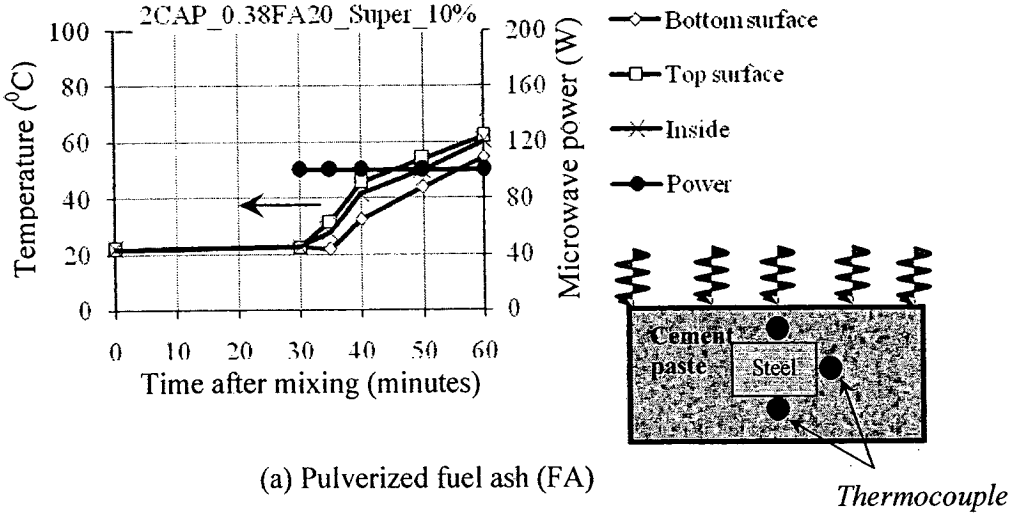

(a) Pulverized fuel ash (FA)

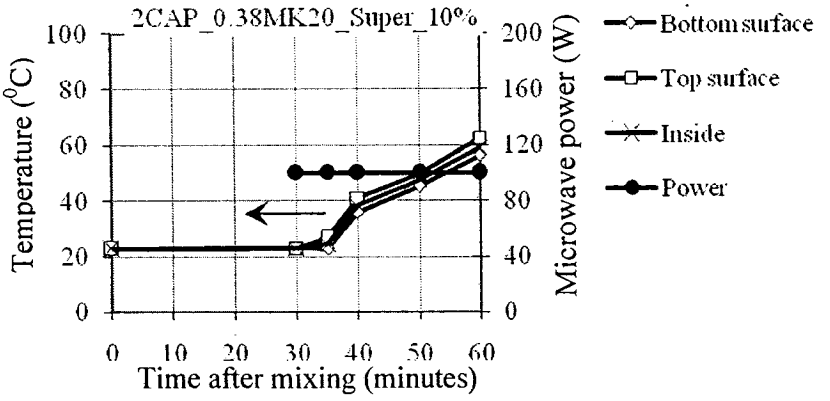

(b) Metakaolin (MK)

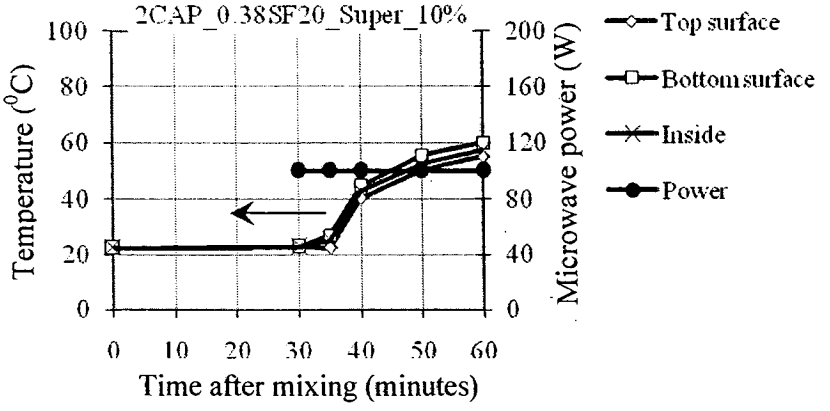

(c) Silica fume (SF)

Fig. 4.10 Temperature and power history during applying microwave energy of various cement pastes mixed with pozzolan materials.

The typical micrographs of FA–cement, MK–cement, and SF–cement pastes at the age of 4 hours after mixing and curing by wrapping with a plastic sheet; at 28 days after curing in lime-saturated deionized water; and after being subjected to microwave energy at a microwave power of 100 watt for 30 minutes are shown in Fig. 4.11. The FA–cement paste shows little difference among the microstructures at the three detecting times. Some small fibers appear at the age of 4 hours, but none appear in the FA–cement paste that was heated by microwave energy. The MK–cement paste, shows little difference between the normal-cured and microwave-cured pastes. On the other hand, for the SF–cement paste the SF particles under microwave curing have dispersed more than with the 4-hours normal curing, while the paste at 28 days looks like a plate of C–S–H in which SF particles cannot be distinguished.

Fig. 4.12 shows the atom ratio of Si/Ca versus Al/Ca for the pastes after microwave power of 390 watt had been applied for 45 minutes. It can be seen that in the case of the normal paste (×), the cluster of Si/Ca versus Al/Ca takes place in the narrow range of the Si/Ca ratios equal to 0.220–0.263 while the Al/Ca ratios equal to 0.079–0.091. The paste mixed with FA (CAP_0.38FA20_Super_10%,) has a wider dispersion of Si/Ca versus Al/Ca than does the normal paste. In the paste mixed with MK (2CAP_0.38MK20_Super_10%), the Si/Ca versus Al/Ca has shifted to achieve a higher Al/Ca ratio in comparison with the normal paste. In the SF paste (2CAP_0.38SF20_Super_10%), the Si/Ca versus Al/Ca shifted to achieve a higher increase in the Si/Ca ratio in comparison with the normal paste. These phenomena can be explained by noting that the chemical composition of FA shows a higher aluminum oxide content than does Portland cement and the effect of this composition is higher than that of the MK–paste. On the other hand, SF is a silica-rich material; therefore, the Si/Ca ratios in the SF–paste are shifted from 0.582 to 1.184. It appears, therefore, that microwave energy can expand the dispersion of silica in an SF paste. Nevertheless, this dispersion has a wide range, that of 0.563 to 1.163.

(a) 2CAP_0.38FA20_ Super_10% at the age of 4 hours

(b) 2CAP_0.38MK20_ Super_10% at the age of 4 hours

(c) 2CAP_0.38SF20_ Super_10% at the age of 4 hours

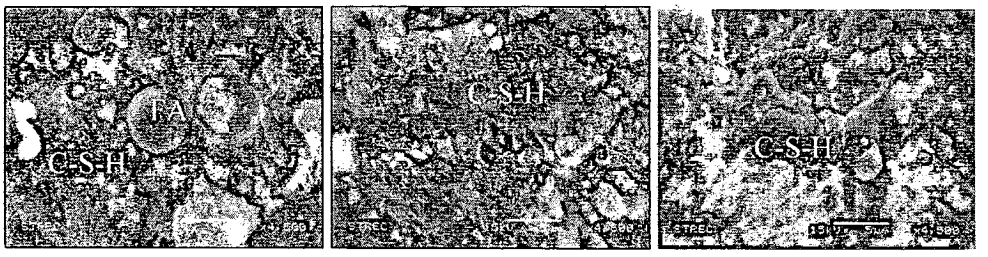

(d) 2CAP_0.38FA20_ Super_10% at the age of 28 days

(e) 2CAP_0.38MK20_ Super_10% at the age of 28 days

(f) 2CAP_0.38SF20_ Super_10% at the age of 28 days

(g) 2CAP_0.38FA20_ Super_1% after applying microwave energy power 100 watt for 30 minutes

(h) 2CAP_0.38MK20_ Super_1% after applying microwave energy power 100 watt for 30 minutes

(i) 2CAP_0.38SF20_ Super_1% after applying microwave energy power 100 watt for 30 minutes

Fig.4.11 Micrographs of various cement pastes mixed with pozzolan materials with different water-to-cementitious ratios at 4 hours subjected to normal curing (lime-saturated deionized water) and microwave energy.

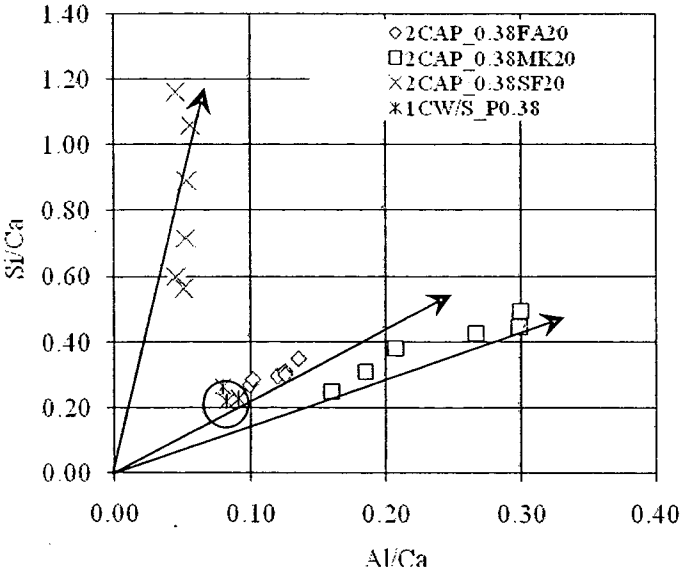

Fig.4.12 Atom ratio of Si/Ca versus Al/Ca for the pastes of 2AP_0.38FA20, 2CAP_0.38MK20 and 2CAP_0.38SF20 after applying microwave power 100 watt for 30 minutes.

X-ray diffractometry was used to determine the degree of crystallinity of the hydrated cement products and the existence of crystalline coexisting phases. Fig. 4.13 shows X-ray diffraction of CAP_0.38FA20_Super_1%, 2CAP_0.38MK20_Super_1% and 2CAP_0.38SF20_Super_1% after MW power of 390 watt had been applied for 45 minutes. The phases identified include calcium silicate hydrate (Ca_3SiO_5), calcium hydroxide ($Ca(OH)_2$), residual lime (CaO), and Xenotile ($Ca_6(SiO_3)_6(H_2O)$).

As shown in Fig. 4.13, in regard to the effect of pozzolan material on the phase characteristics of CAP_0.38FA20_Super_1%, 2CAP_0.38MK20_Super_1%, and 2CAP_0.38SF20_Super_1% after microwave power of 390 watt had been applied for 45 minutes, the calcium silicate hydrate (Ca_3SiO_5) and calcium hydroxide ($Ca(OH)_2$) phases are similar.

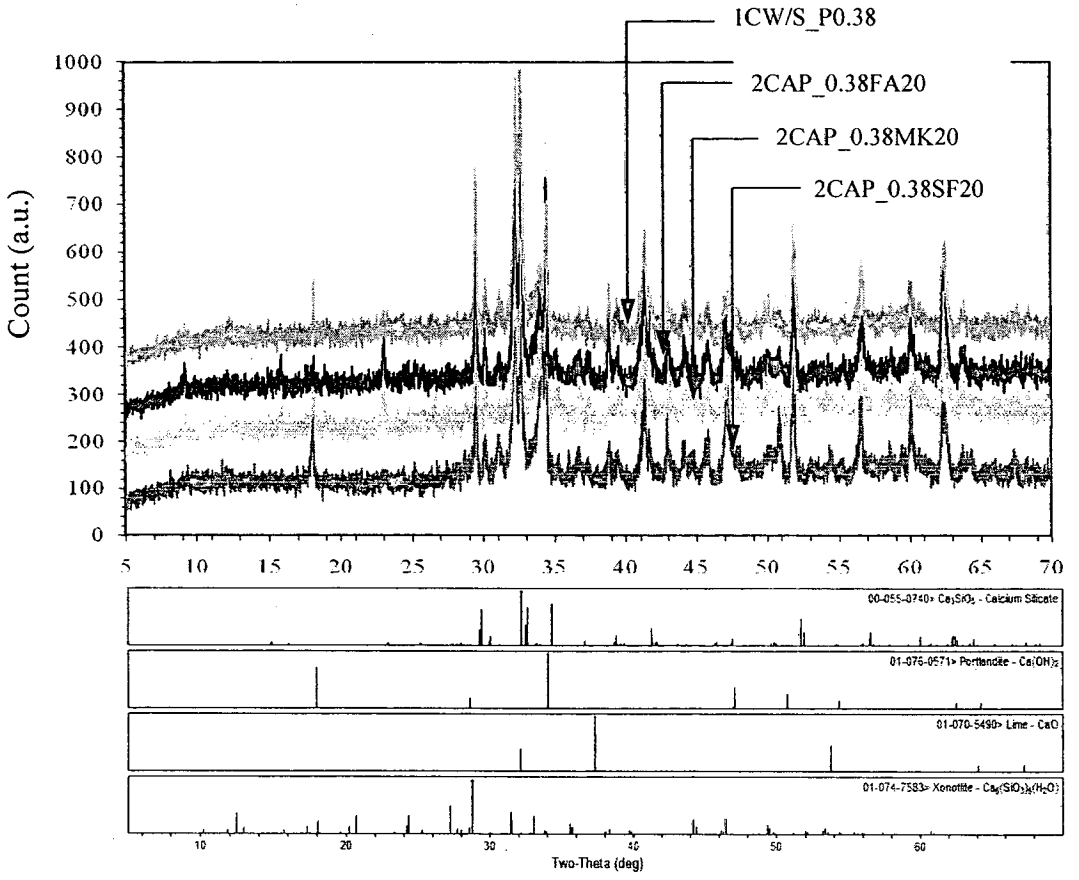

Fig. 4.13 X-ray diffraction of 2CAP_0.38FA20, 2CAP_0.38MK20 and 2CAP_0.38SF20 after applying microwave power 100 watt for 30 minutes.

The compressive strength of the CAP_0.38FA20_Super_1%, 2CAP_0.38MK20_Super_1%, and 2CAP_0.38SF20_Super_1% pastes after the application of microwave power of 376 watt for 45 minutes compared to compressive strength under normal curing conditions are shown in Fig. 4.14. It was found that when cured at elevated temperatures, the pastes developed strength quite rapidly, especially the SF–cement paste. At the age of 8 h after microwave curing the FA–cement paste gained a compressive strength of 4.1 MPa (41000 % higher than that of the normal-cured paste); at 24 hours curing, FA–cement pastes showed a compressive strength of 9.2 MPa, and at 7 and 28 days the strengths were 25.1 and 40.6 MPa, respectively. For the elevated temperature curing with the MK– and SF–cement pastes, the strength obtained at 8 hours was 8.6 and 12.1 MPa, which exceeded the strength of the non-microwave-cured pastes. The pastes containing pozzolan material showed strength development behaviors that differed from those of the normal paste; that is it can develop continuously the strength after 24 hours and later ages. This is due to the pozzolan reaction, which produces the secondary C–S–H content and the hydration reaction (Massazza,

2003); these effects contribute to the heat generated by the microwave and the heat liberated from hydration which, in turn, contribute to the later-age strength development of the pozzolan pastes.

The compressive strength development of the pozzolan pastes relate to their $Ca(OH)_2$ content: that is, strength development is related to the weight loss of the sample in the range of 400–550 ^{0}C, the weight loss is converted to $Ca(OH)_2$ and then added to the $Ca(OH)_2$ that has been carbonated. Fig. 4.15 shows that the $Ca(OH)_2$ content of the FA–, MK–, and SF–cement pastes were 3.08, 2.36, and 1.59 (%wt.), respectively. This illustrates that the that the SF–cement paste consumed more $Ca(OH)_2$ in the pozzolan reaction and produces more C–S–H, the combination of which means that of the three pastes, this one achieves the highest compressive strength.

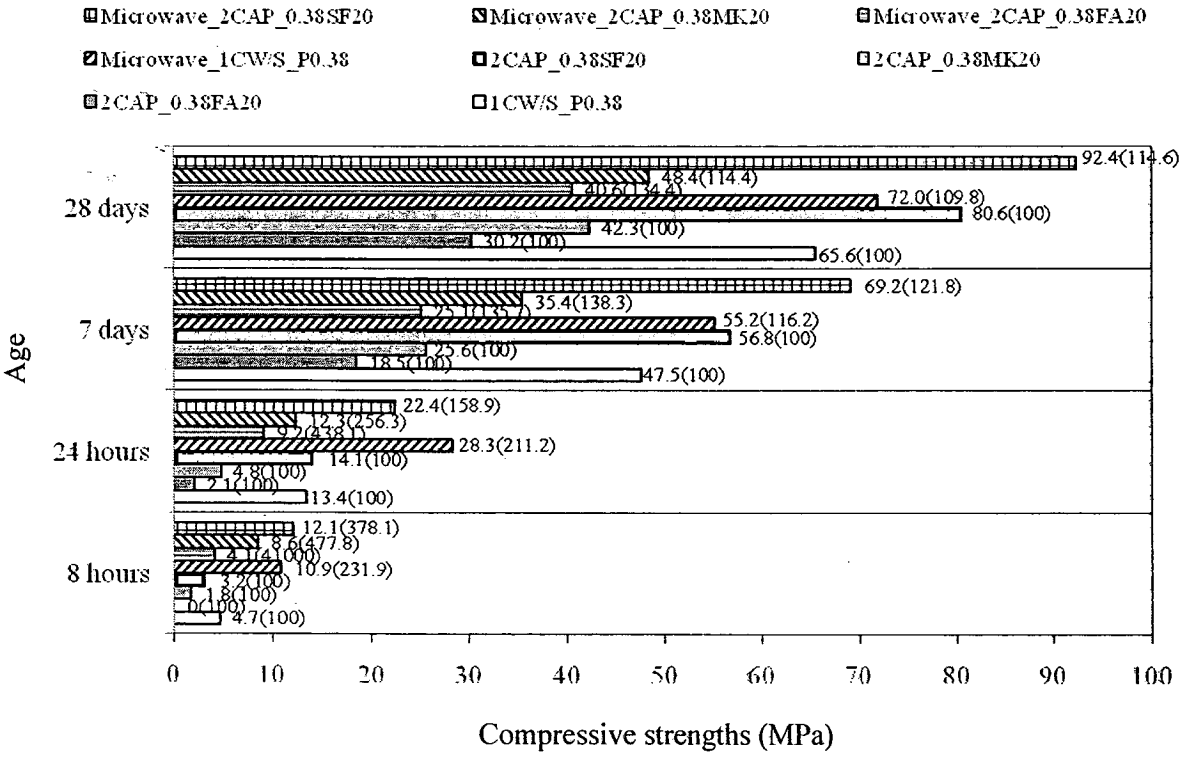

Fig. 4.14 Compressive strengths of the pastes of CAP_0.38FA20, 2CAP_0.38MK20 and 2CAP_0.38SF20 after applying microwave power 100 watt for 30 minutes compared to normal curing.

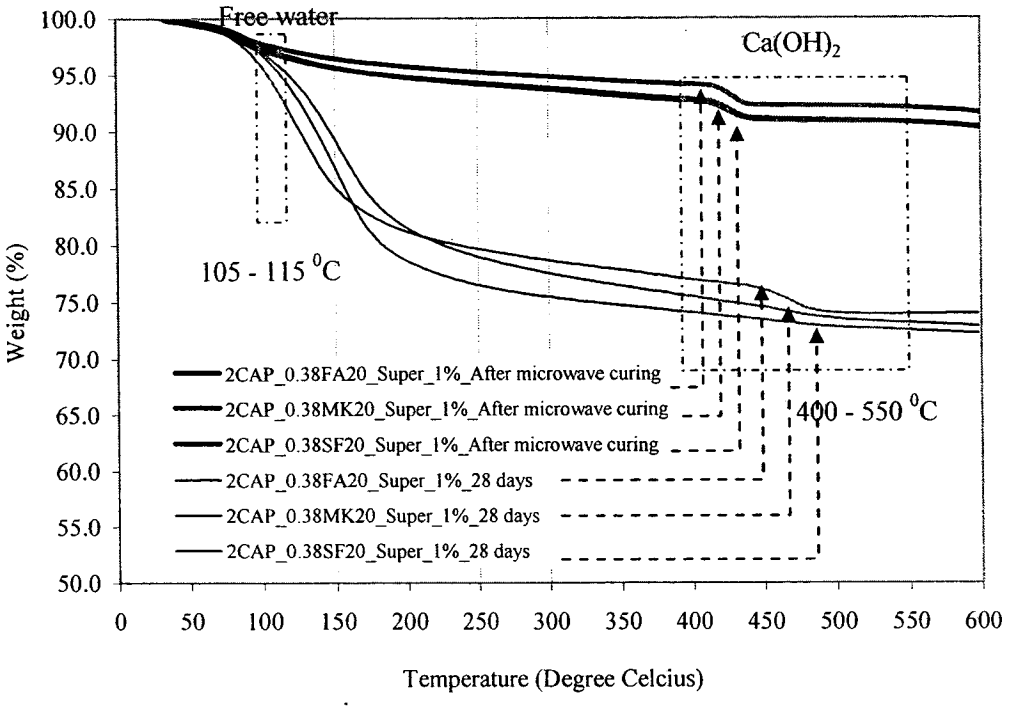

Fig. 4.15 Thermal analysis results by comparison among among different temperatures and weights of the pastes with/without pozzolan materials.

4.4.2.3 Reinforced mortar and concrete

Fig. 4.16 shows the temperature increases and microwave power used throughout the curing time of the mortar (3CAM0.38_1:2.75) proportioned with Portland cement Type I: Ottawa sand at 1: 2.75 by weight and water-to-cement mass ratio of 0.38. The temperatures increases are related to increases in of microwave power. This is because the heat generated by microwave energy varies in correspondence with the electric field intensity ($\bar{E}$), as shown in Eq. (2.19). In other words, when the microwave power increases, so too does the intensity of the electric field. Moreover, the temperature behaves similarly for all the monitored points. In terms of dielectric behavior, the SiO_2 in sand does not absorb microwave energy; therefore, the heat that accrues from microwave energy proceeds from hydration of the cement particles and water molecules.

Regarding the rate at which the temperature increases, in the first period during which microwave is introduced inwards to the microwave-cured mortar, the rate of increase is higher than that of the later period. This is because during the first period, the abundance of water inside the mortar consistently affects increases in the amount of heat generated. On the other hand, during the later period the water's composition changes to C–S–H and is evaporated outward, which causes a gradual reduction in the amount of heat generated as the amount of available water, especially free water, decreases.

It was found that the rate at which temperatures increases at the end of curing, corresponds to the power level of the microwave energy applied. For example, at the top surface where water evaporation take place, the final temperature at microwave power levels 50, 100, and 150 watt run at 69 ^{0}C, 123 ^{0}C, and 190 ^{0}C, respectively. This shows that though the microwave power level was increased up to two times, the temperature does not raise a half of the microwave power level. This high rate of heat generation at high power levels directly increases more rapidly the rate at which the temperature of the heated mortar increases. In addition, the temperature as immediately generated can accelerate hydration; that is, this reaction also generates heat.

A comparison of the differences in the temperature increases of the microwave-cured paste (Fig. 4.16) and the microwave-cured mortar at the same water-to-cement mass ratio shows that the mortar stores less energy than does the paste. This is due to high specific heat of sand (664 J/kg-^{0}C) [127], which causes the temperature of mortar rises up at a lower rate. Furthermore, as water evaporates from the cement paste, its temperature decreases more rapidly than does the of the mortar sample.

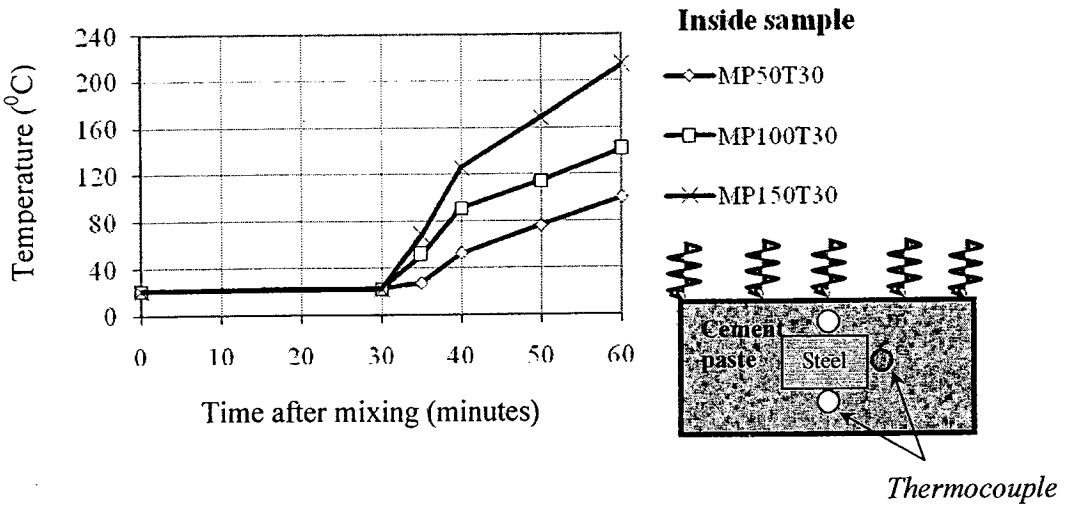

Fig. 4.16 Temperature and power history during the application of microwave energy to an inside of the mortar sample (3CAM0.38_1:2.75) with different microwave power levels.

Fig. 4.17 shows the temperature and power history during the application of microwave energy to a concrete (3CAC0.38_1:1:1) with different microwave power levels. The concrete is proportioned as follows: Portland cement : Ottawa sand : crushed limestone rock equal to 1:1:1. This temperature behavior differs in clear ways from the temperature behavior observed in the mortar. In detail, during the early period of microwave curing the temperature increases rapidly; that is, it rises by an average of every 5 minutes. Subsequently, the temperature increases at a constant rate. All the monitored points—the top surface, bottom surface, and inside—behave similarly in this regard, which indicates that the presence of crushed lime stone rock affects the rate at which the temperature increases as well as the final temperature achieved. This may be because crushed limestone rock has a rough surface to which it is easier for water molecules to attach than the smoother surface of Ottawa sand [128]. This result shows that the heat generated within this sample is lower than that of is generated in the mortar sample. This means that when microwave energy is introduced to the concrete sample, the sample maintains temperature or absorbs heat better than does the mortar under similar conditions.

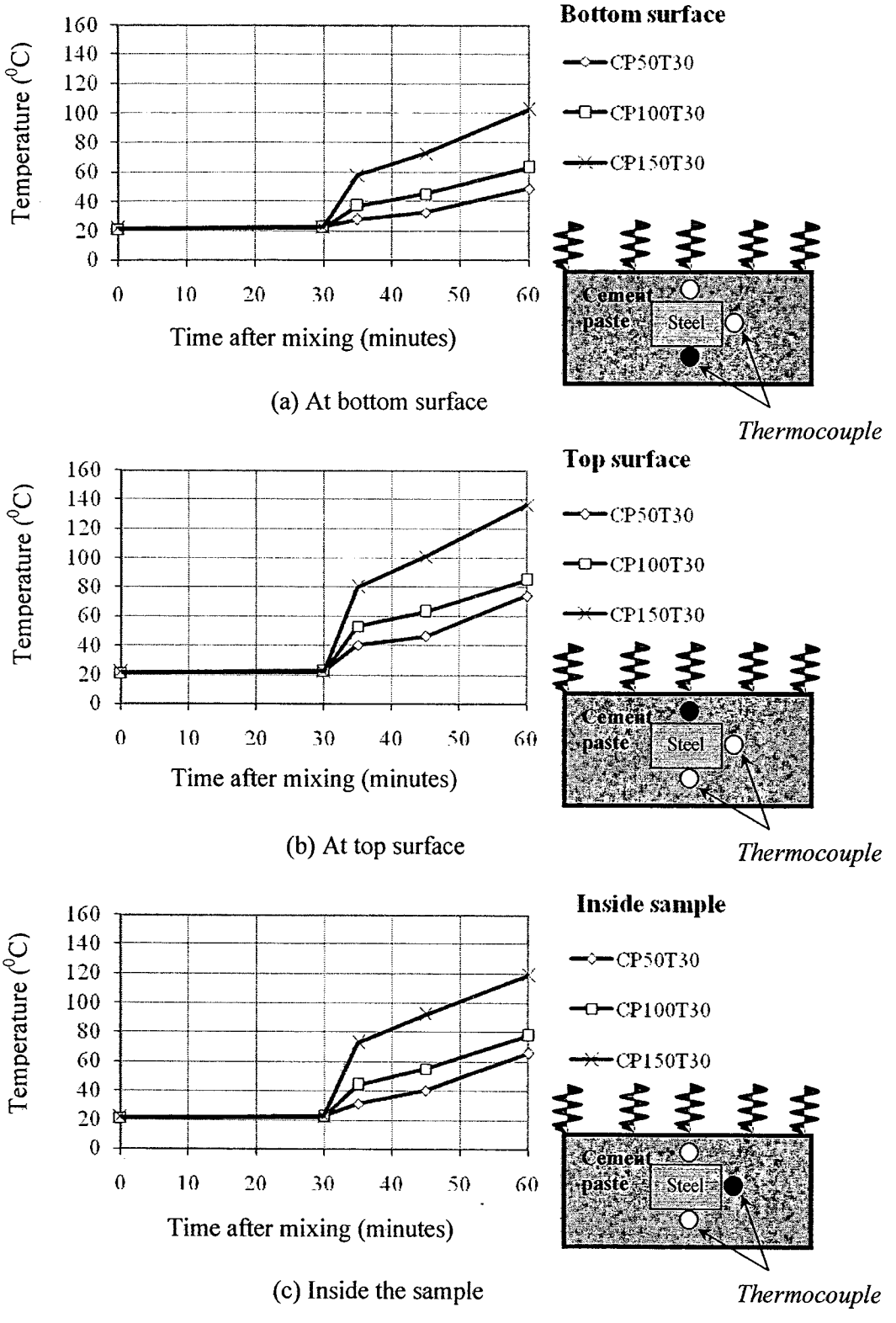

Fig. 4.17 Temperature and power history during the application of microwave energy to concrete (3CAC0.38_1:1:1) with different microwave power levels.

Typical micrographs of the mortar (3CAM0.38_1:2.75) subjected to microwave energy, and concrete (3CAC0.38_1:1:1) subjected to microwave energy at 50 watt for 30 minutes are shown in Fig. 4.18. It is not clearly seen from Fig. 4.18(a) and 4.18 (f) that the samples consist of hydrated phases and pores. On its surface, the large particles appear to be agglomerated with a small particle, especially in the microwave-cured concrete.

The EDX results for the cement pastes subjected to microwave energy are shown in Fig. 4.19: The atom ratio of Si/Ca versus Al/Ca for the pastes of (1CW/S_P0.38) after the application of microwave power of 100 watt for 30 minutes shows that for the normal paste, the Si/Ca cluster versus the Al/Ca cluster takes place in the narrow range of Si/Ca 0.163–0.240, but with a wider range of Al/Ca equal to 0.022–0.090. In the mortar and concrete, the degrees of scatter for Si/Ca versus Al/Ca are greater than those of the other pastes. It is likely that the aggregate of the paste affects the distribution of the Si, Ca, and Al elements, causing them to become more widely dispersed.

(a) 3CAM0.38_1:2.75 at a microwave power 50 watt

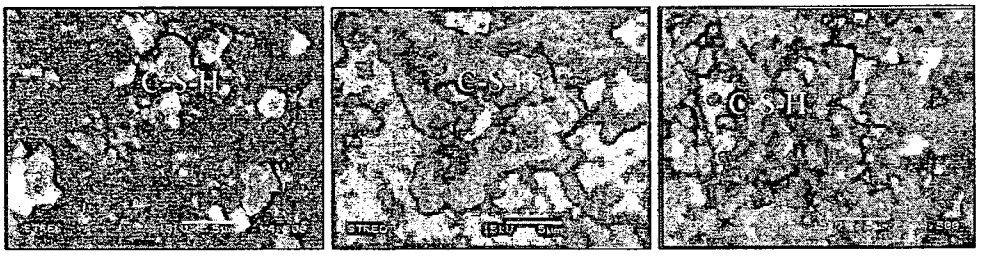

(b) 3CAC0.38_1:1:1 at microwave power 50 watt

(c) 3CAC0.38_1:1:1 at microwave power 100 watt

(d) 3CAC0.38_1:1:1 at microwave power 150 watt

Fig. 4.18 Micrographs of mortar and concrete with different microwave power levels.

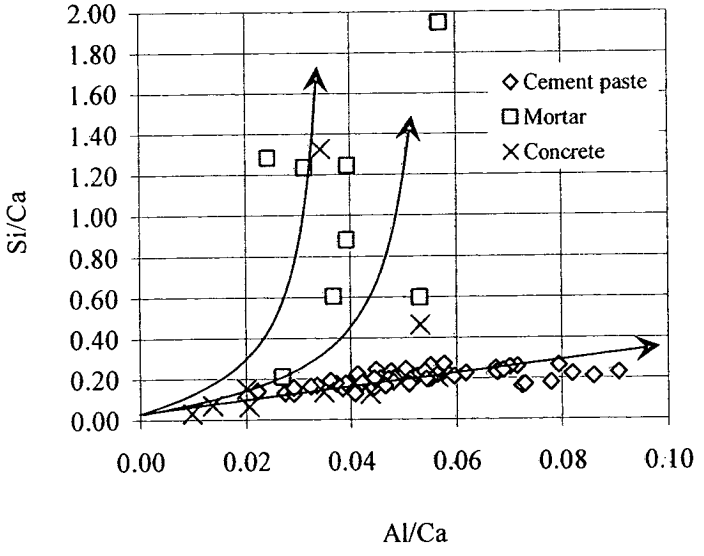

Fig. 4.19 Atom ratio of Si/Ca versus Al/Ca of cement paste, mortar and concrete after applying microwave energy with different power levels.

Figs. 4.20 and 4.21 show the X-ray patterns of the hydrated products in the mortar and concrete after microwave power of 100 watt had been applied for 30 minutes. For mortar, the phases identified include hatrurite (Ca_3SiO_5) and lanite (Ca_2SiO_4). Similar to mortar, the concrete consists mainly of hatrurite (Ca_3SiO_5) and quartz (SiO_2).

The compressive strengths of the mortar of (3CAM0.38_1:2.75) when subjected to microwave energy, and concrete (3CAC0.38_1:1:1) compared to normal curing are shown in Fig. 4.22: when cured at elevated temperatures using an microwave power level of 180 watt, mortar can develop strength quite rapidly, and with a higher microwave power level the development of strength decreases. It could be that an increase in microwave power significantly affects the interfacial transition zone between the neat paste and the aggregate [129]. From the literature, increases in temperature expand the range of the interfacial transition zone and as a consequence compressive strength is reduced.

Similar to the mortar case, the microwave-cured concrete corresponds to the microwave power level shown in Fig. 4.23, the compressive strength of concrete decreases with increases in the power level, as previously discussed earlier.

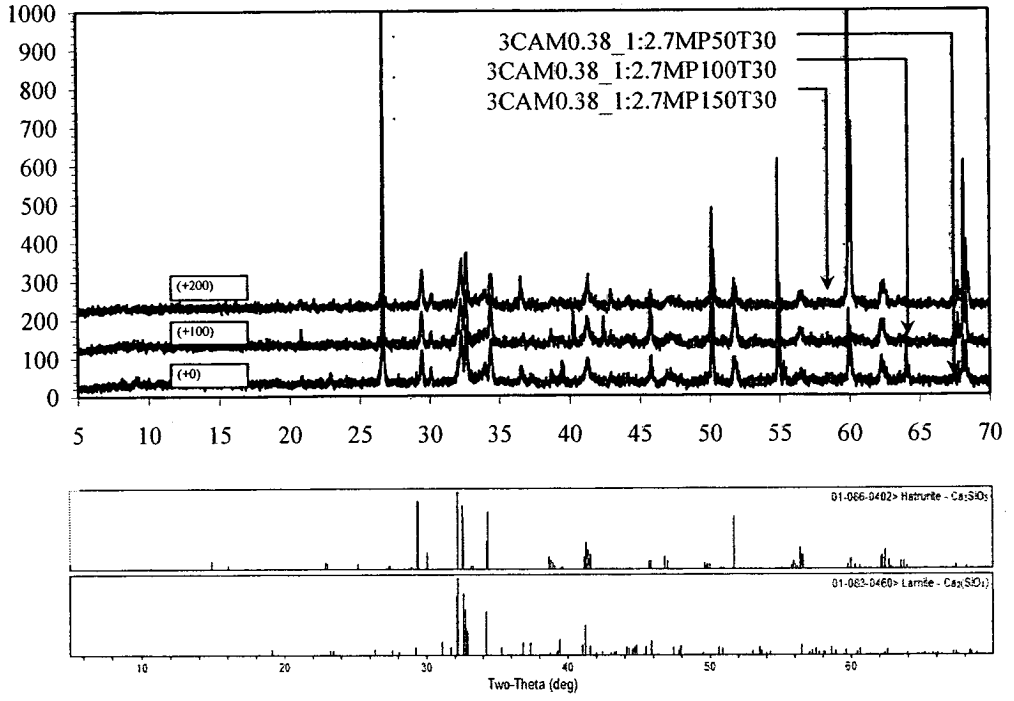

Fig. 4.20 X-ray diffraction of mortar after applying microwave energy with different power levels.

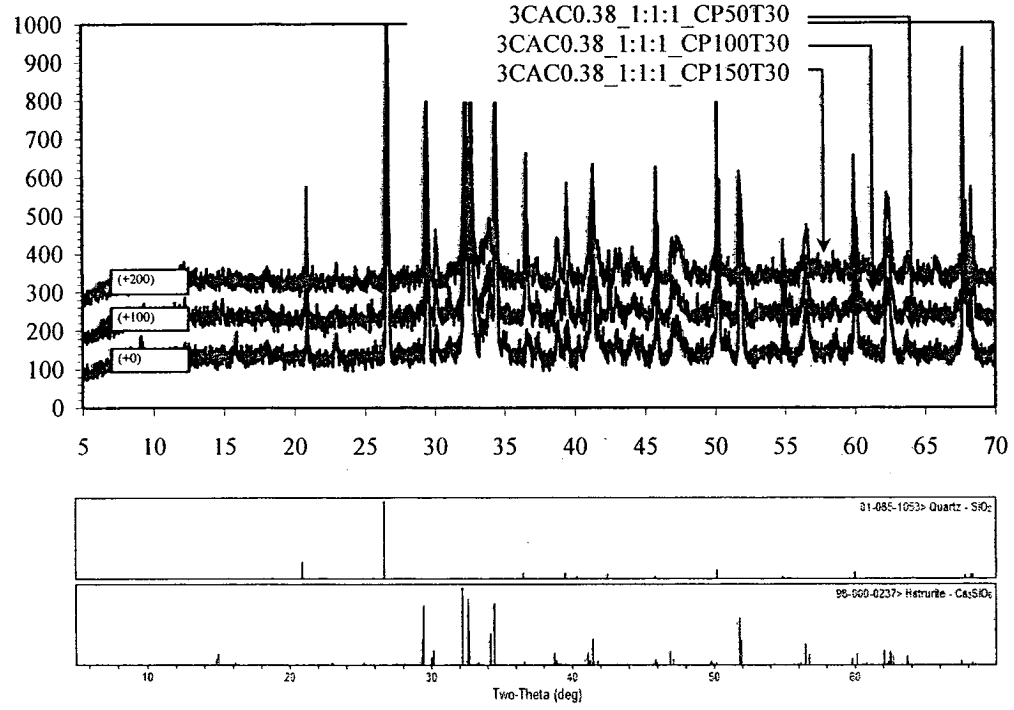

Fig. 4.21 X-ray diffraction of concrete after applying microwave energy with different power levels.

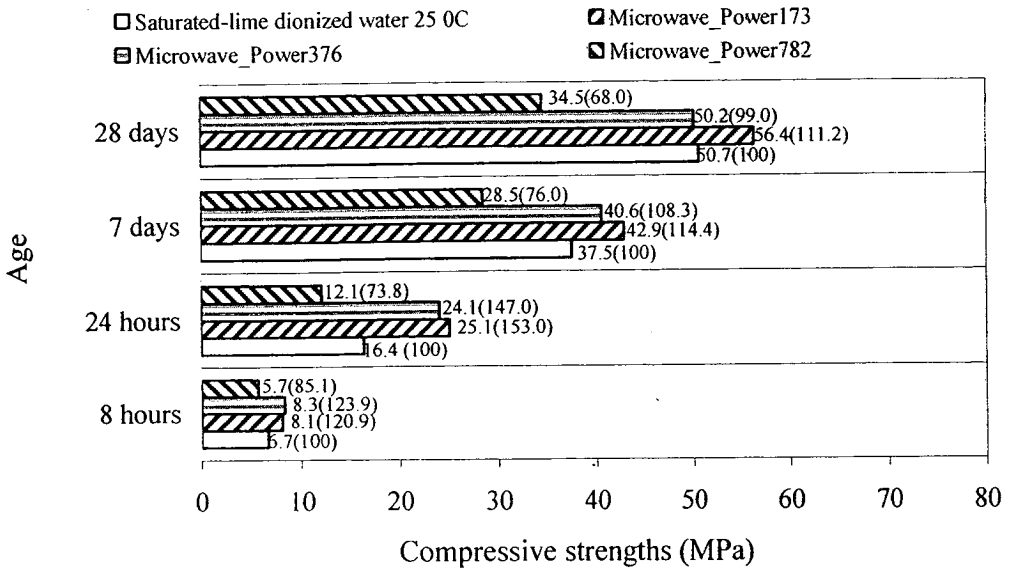

Fig. 4.22 Compressive strengths of mortar after applying microwave energy with different power levels.

or

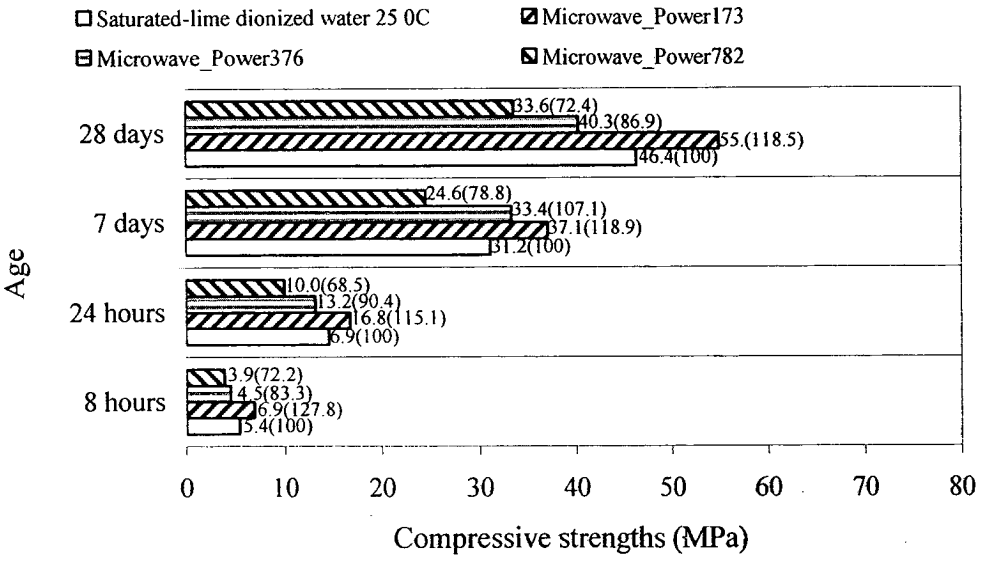

Fig. 4.23 Compressive strengths of concrete after applying microwave energy with different power levels.

4.4.3 Effects of microwave processing

4.4.3.1 Delay times

This section discusses the effects of delay times. Basically, the delay time is the time that elapses after mixing has finished and before the application of microwave energy has begun. The delay time comprises the dormant period, during which the hydration reaction slow down; the initial setting time, during which the mix begins to take on a form, and the final setting time, the point at which the structure has formed. Specific delay times are expected to affect various properties in particular ways. For example, if microwave were applied at the final setting time, pore content would be expected to increase so that microcracking would take place in the paste to be cured.

Figs. 4.24–5.35 show the temperature profile against the application times for reinforced cement paste, FA–cement paste, MK–cement paste, and SF–cement paste at water-to-solid mass ratio (w/s) of 0.38 with various delay times when subjected to a microwave power level of 100 watt for 30 minutes. In the case of the plain cement paste (Fig. 4.24), microwave energy applied to the sample at a delay time of 30 minutes caused the highest temperature rise in the pastes to be processed—a result of the high water content especially the free water content within the sample. Because of the high water content, the sample at 30 minutes was able to absorb a large amount of energy and convert it easily into heat [4,5]. However, applications at the initial setting time tended to decrease the extent to which the temperature rose due to the free water used in the hydration reaction and then combined in the C–S–H structure. However, even so, when microwave energy was applied at the final setting time the temperature increased to a greater extent than it had during the initial setting time. These relative increases can be accounted for by the fact that at the initial setting time point, temperature rise accrues from the initial state of the heat liberated from the hydration reaction, while at the final setting time temperature rise accrues from the approaching hydration peak, which sustains the heat generation from hydration. As a result, the temperature rise at the final setting time is higher than that of taking place at the previous initial setting time.

The cement pastes mixed with FA (Fig. 4.25), MK (Fig. 4.26), or SF (Fig. 4.27) showed a similar tendency in regard to temperature rise as that of the reinfoced cement paste. However, for all these mixes, the temperature rise at the final setting time was lower than that for the pastes at the initial setting time. The reason for this is that the materials used to replace the pozzolan material caused heat liberation to occur because of hydration is delayed more than the pozzolan used in the plain paste.

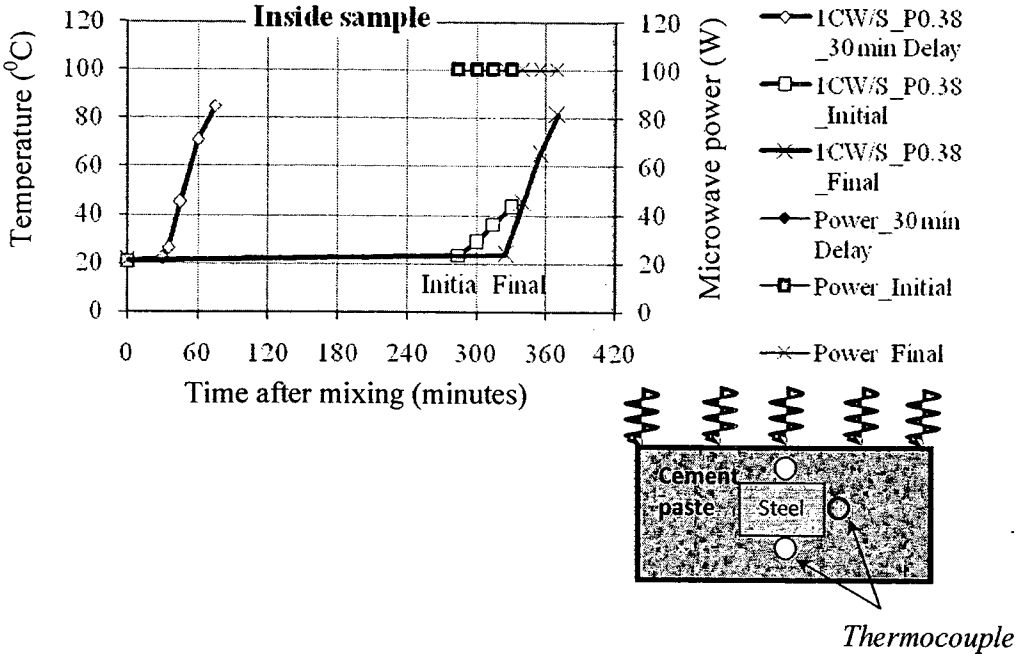

Fig. 4.24 Temperature and power history during applying microwave energy of reinforced cement pastes at a water-to-solid material of 0.38 with vary delay times.

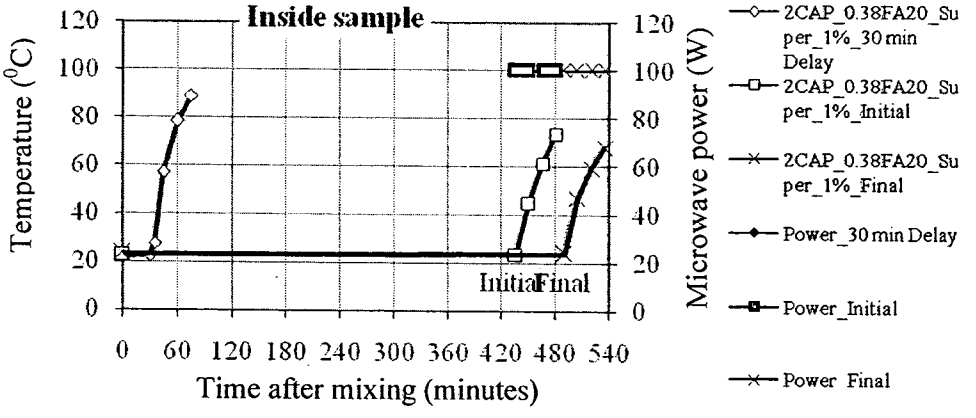

Fig. 4.25 Temperature and power history during applying microwave energy of reinforced FA- cement paste at a water-to-solid material of 0.38 with vary delay times.

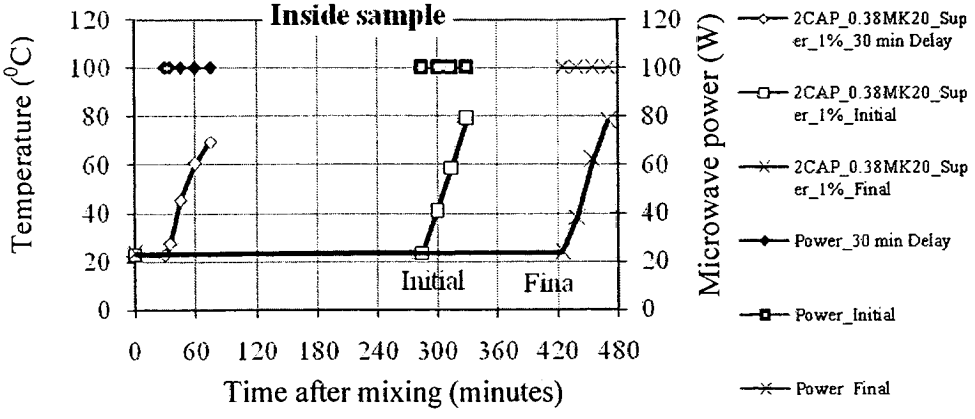

Fig. 4.26 Temperature and power history during applying microwave energy of reinforced MK-cement pastes at a water-to-solid material of 0.38 with vary delay times.

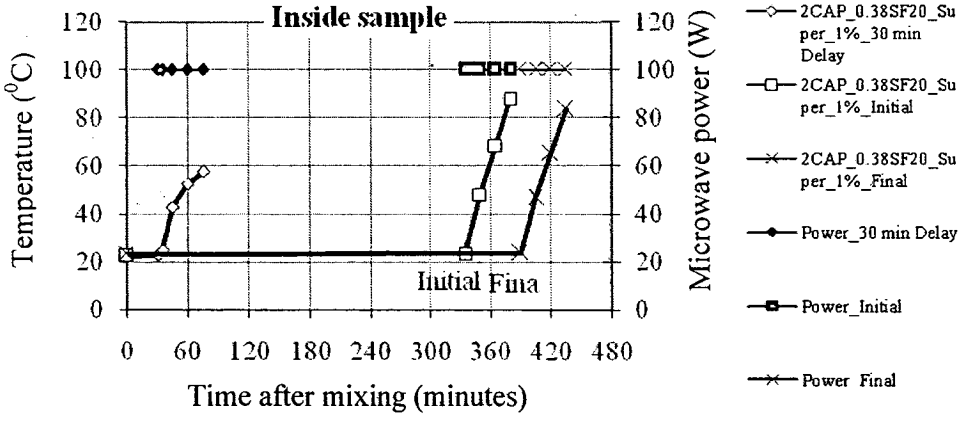

Fig. 4.27 Temperature and power history during applying microwave energy of reinforced SF-cement pastes at a water-to-solid material of 0.38 with vary delay times.

Typical micrographs of the plain cement paste (1CW/S_P0.38), FA–cement paste, MK–cement paste, and SF–cement paste when subjected to microwave energy at an microwave power level of 100 watt for 30 minutes are shown in Fig. 4.28. Formed when microwave energy was applied at the final setting time, ettringite appears on the surface of the plain cement paste [130]. On the other hand, the pozzolan paste showed no difference between the initial and final setting time of the microwave application.

From the EDX results for plain cement paste subjected to microwave energy are shown in Fig. 4.29. The atom ratio of Si/Ca versus Al/Ca for the pastes of (1CW/S_P0.38) to which microwave power of 100 watt was applied for 30 minutes, agglomerated and tended to show an increase in the Al/Ca ratio [131], indicating that microwave energy can cause Al-

element distribution [132]. For the FA–cement paste, the distribution of Al/Ca ratio showed a narrower range than that did that of the plain paste [133]. In the MK–cement paste, the distribution was wider than it was in the plain paste because of a major constituent of MK is aluminum. While the SF in SF–paste consists mainly of Si-element.

Figs. 4.30 – 4.33 show the effects of delays on the phase characteristics of the 1CW/S_P0.38, CAP_0.38FA20_Super_1%, 2CAP_0.38MK20_Super_1%, and 2CAP_0.38SF20_Super_1% after microwave power of 100 watt had been applied for 30 minutes. The calcium silicate hydrate (Ca_3SiO_5), calcium hydroxide ($Ca(OH)_2$) lime (CaO), and Xenotile phases were found to be similar.

(a) 1CW/S_P0.38 at microwave power 100 watt for 30 minutes and delay time at initial setting time

(b) 2CAP_0.38FA20_Super_1% microwave power 100 watt for 30 minutes and delay time at initial setting time

(c) 2CAP_0.38MK20_Super_1% microwave power 100 watt for 30 minutes and delay time at initial setting time

(d) 2CAP_0.38SF20_Super_1% at microwave power 100 watt for 30 minutes and delay time at initial setting time

Fig. 4.28 Micrographs of various cement pastes at different delay times.

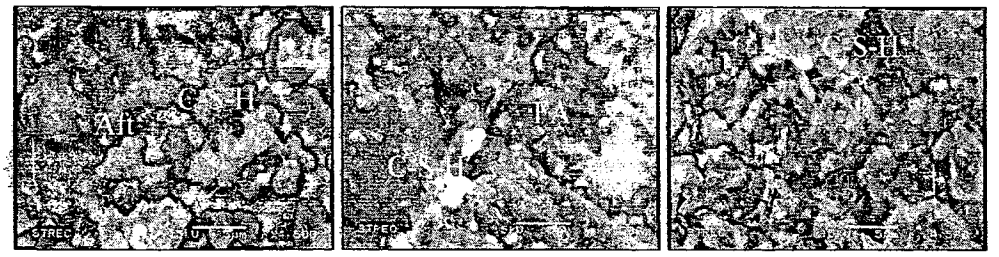

(e) 1CW/S_P0.38 at microwave power 100 watt for 30 minutes and delay time at final setting time

(f) 2CAP_0.38FA20_Super_1% at microwave power 100 watt for 30 minutes and delay time at final setting time

(g) 2CAP_0.38MK20_Super_1% at microwave power 100 watt for 30 minutes and delay time at final setting time

(h) 2CAP_0.38SF20_Super_1% at microwave power 100 watt for 30 minutes and delay time at final setting time

Fig. 4.28 (Cont.) Micrographs of various cement pastes at different delay times.

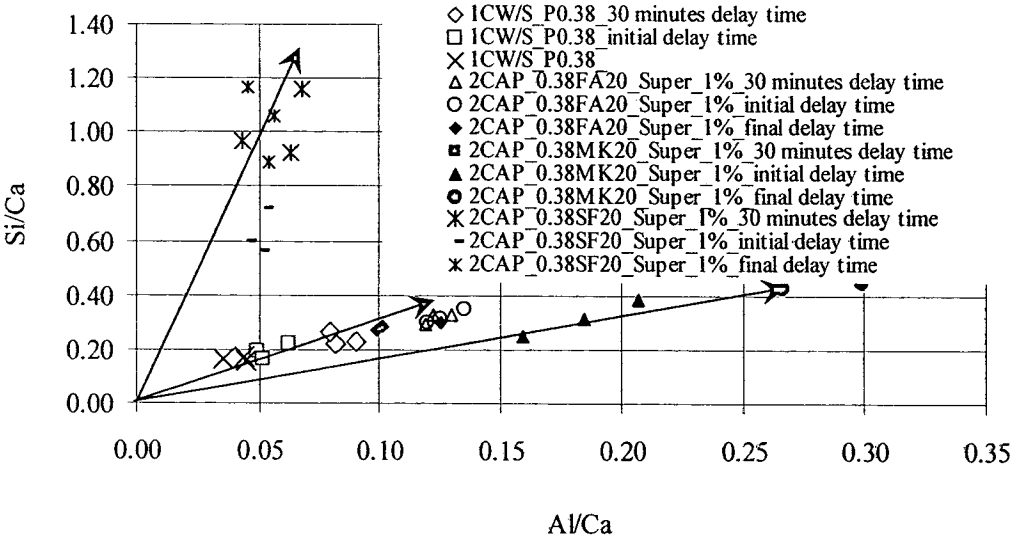

Fig. 4.29 Atom ratio of Si/Ca versus Al/Ca of various cement pastes with different delay times when applying microwave energy.

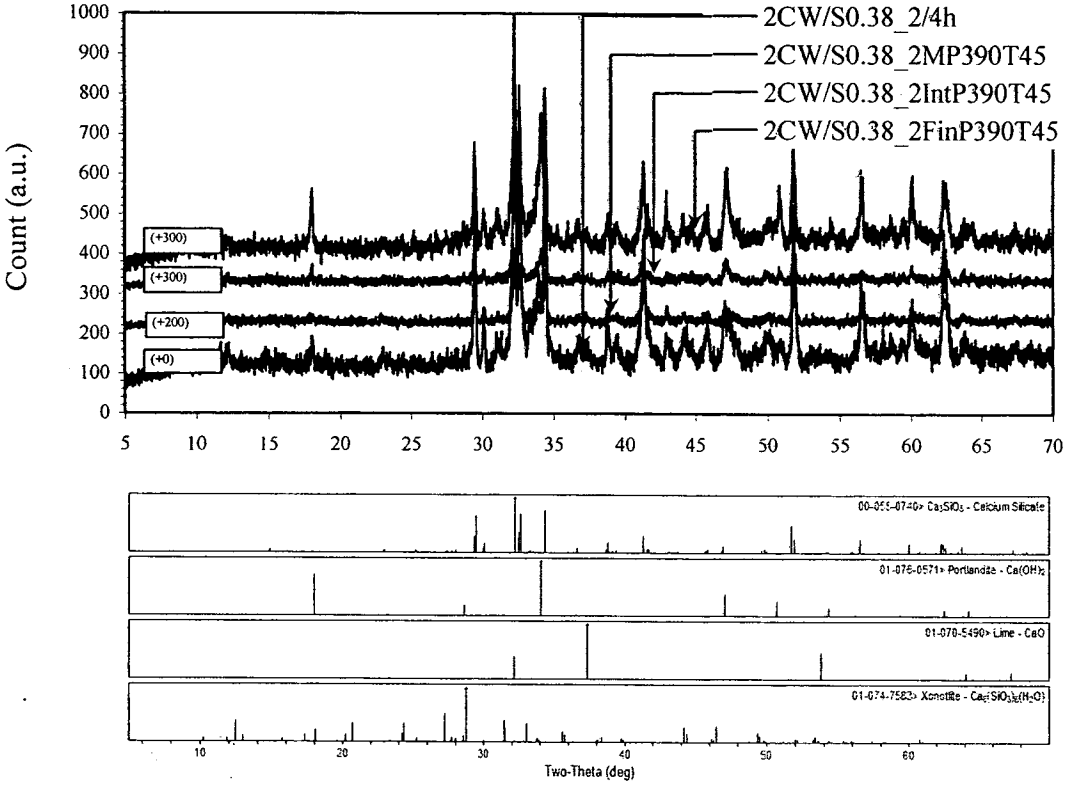

Fig. 4.30 X-ray diffraction of 1CW/S_P0.38 cement paste with different delay times when applying microwave energy.

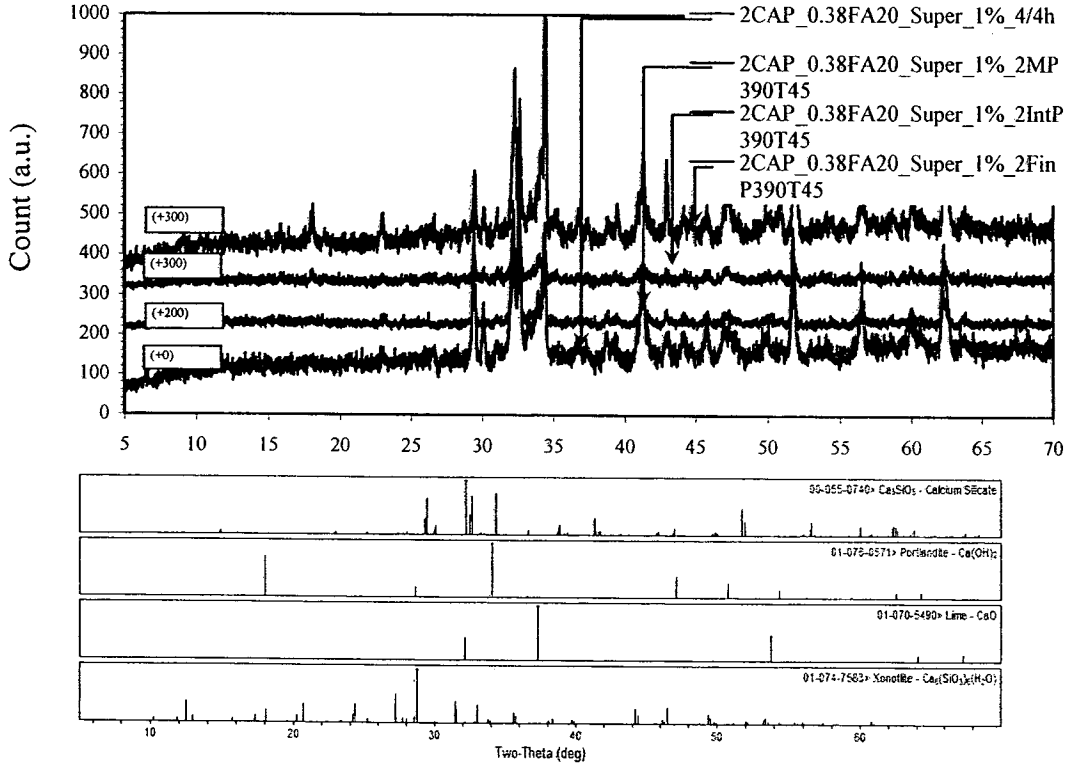

Fig. 4.31 X-ray diffraction of 2CAP_0.38FA20 reinforced cement pastes with different delay times when applying microwave energy.

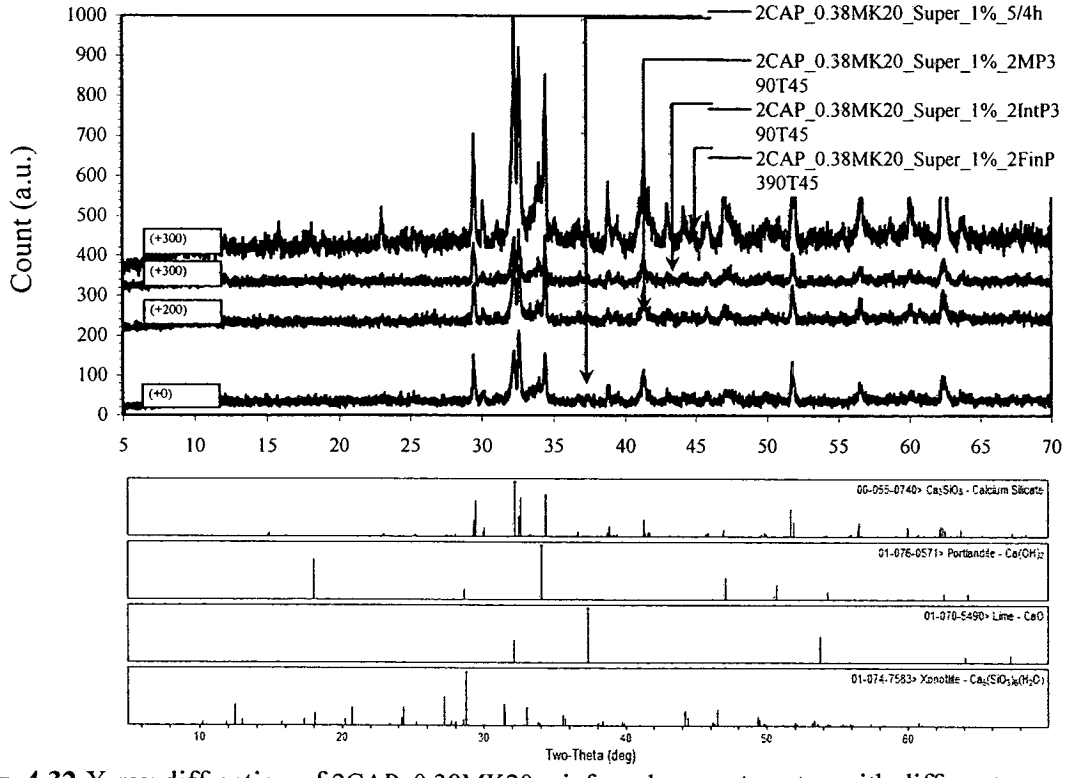

Fig. 4.32 X-ray diffraction of 2CAP_0.38MK20 reinforced cement pastes with different delay times when applying microwave energy.

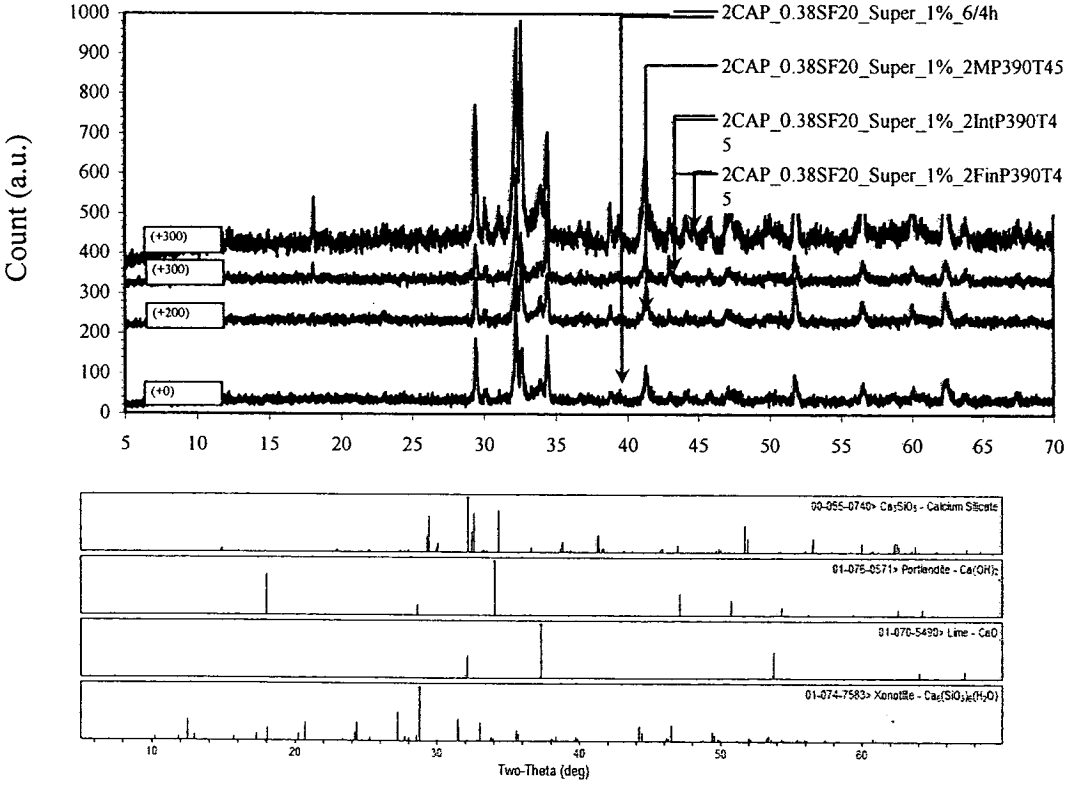

Fig. 4.33 X-ray diffraction of 2CAP_0.38SF20 reinforced cement pastes with different delay times when applying microwave energy.

The compressive strengths of the 1CW/S_P0.38, CAP_0.38FA20, 2CAP_0.38MK20, and 2CAP_0.38SF20 after microwave power of 100 watt had been applied for 30 min are shown in Fig. 4.34. Overall, it can be concluded that using microwave energy for curing beginning at the final setting time can reduce compressive strengths of both early- and late-age reinforced and pozzolan pastes. This is because heat generated by microwave imposed after the C–S–H structure has formed increases the temperature difference between the microstructured paste and the paste during formation, and as a result cracking takes place immediately [71,72]. Moreover, the remaining free water in the capillary pores shows a higher temperature increase than do the hydration products [134] which causes cracking in the internal capillary pores that penetrate the C–S–H structure deeply. Consequently, these effects cause a reduction in the compressive strength of all the pastes.

Fig. 4.35 presents the results of the remaining $Ca(OH)_2$ content of the reinforced cement pastes (1CW/S_P0.38), which are 2.07% (w/w) and 2.34% (w/w) for the initial and final setting times, respectively. These results indicate that applying microwave energy at the final setting time can increase the amount of $Ca(OH)_2$ more so than applying it at the initial setting time. It could be that during the final setting time, the heat generated by microwave in conjunction with the heat of hydration causes an even greater amount of $Ca(OH)_2$.

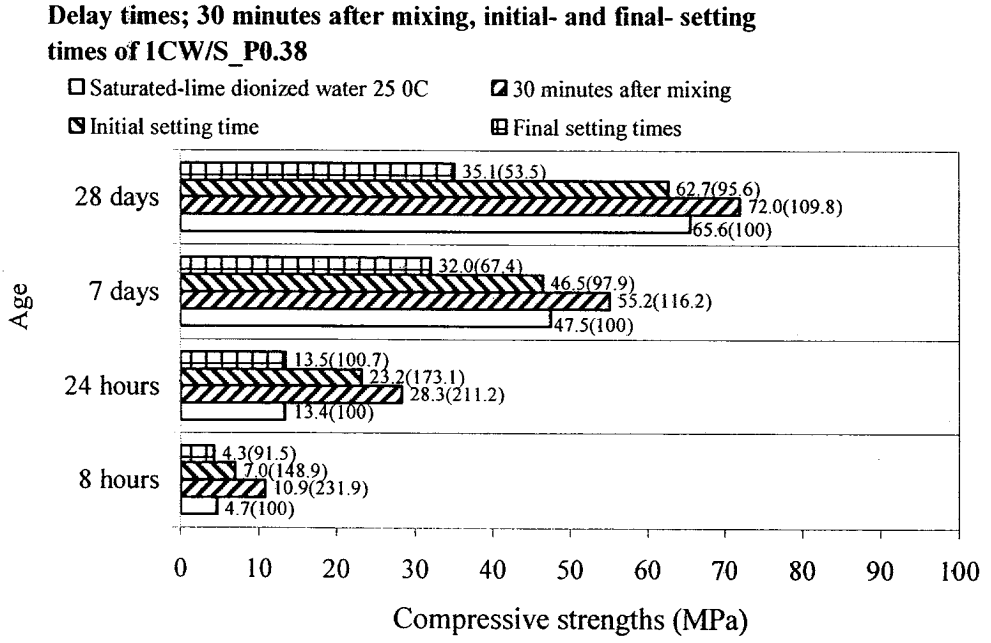

(a) Reinforced pastes

Fig. 4.34 Compressive strengths of 1CW/S_P0.38 reinforced cement paste with different delay times when applying microwave energy.

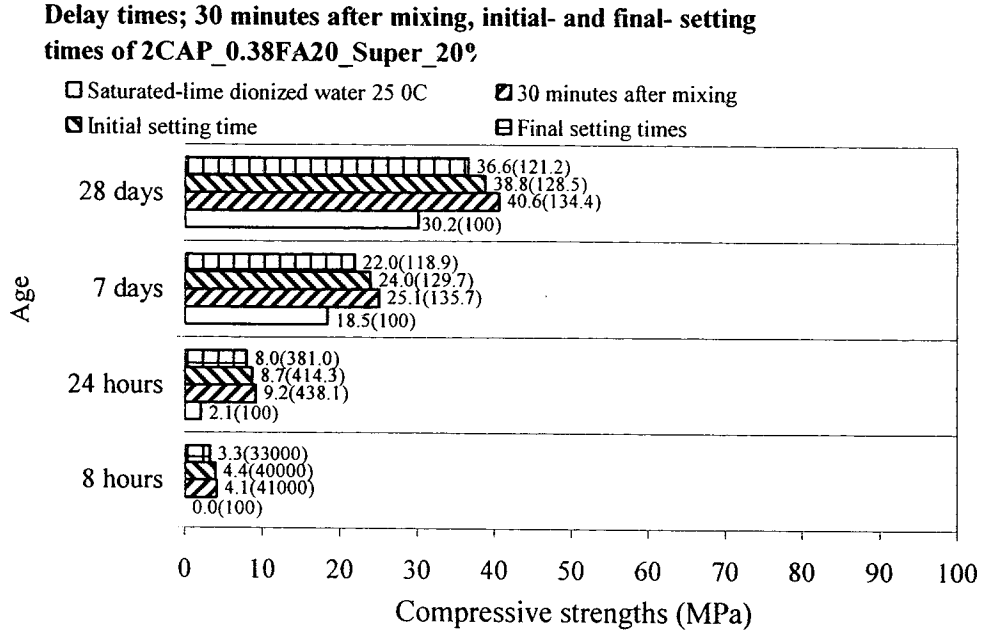

(b) Reinforced pastes mixed with FA

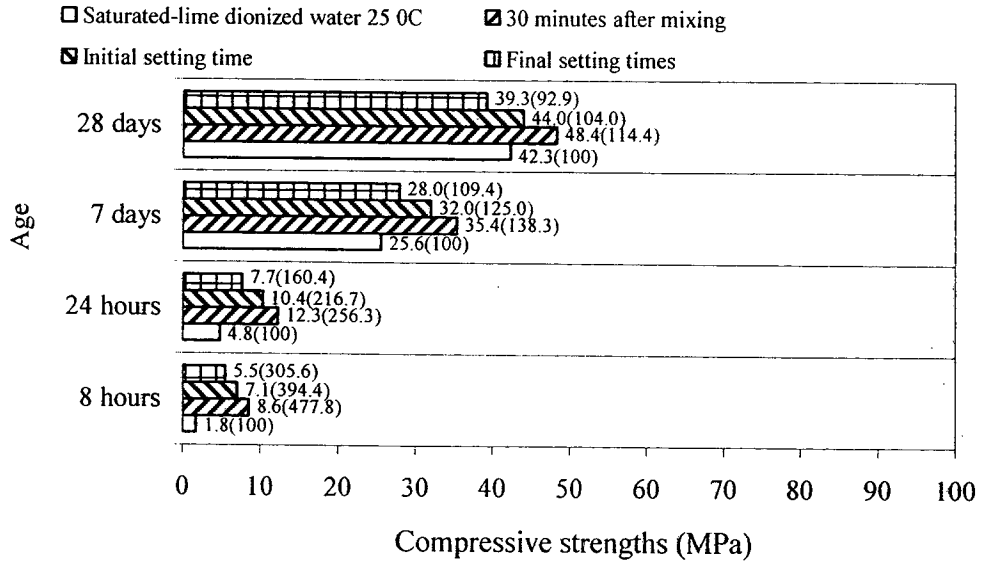

(c) Reinforced pastes mixed with MK

Fig. 4.34 (Cont.) Compressive strengths of 1CW/S_P0.38 reinforced cement paste with different delay times when applying microwave energy.

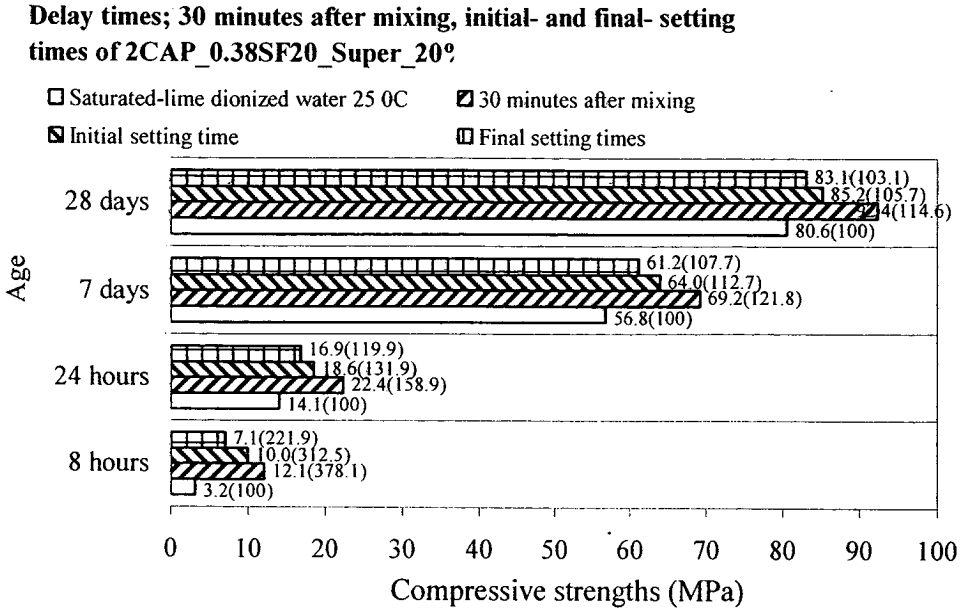

(d) Reinforced Pastes mixed with SF

Fig. 4.34 (Cont.) Compressive strengths of 1CW/S_P0.38 reinforced cement paste with different delay times when applying microwave energy.

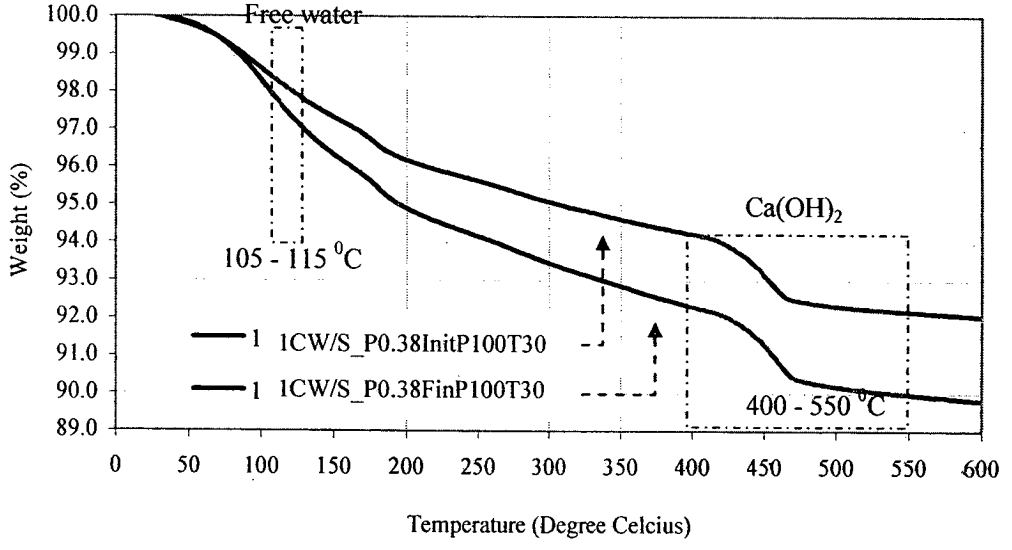

Fig. 4.35 Thermogravimetric analysis (TG) results by comparison among different delay times.

4.4.2.2 Power levels and application times

This section discusses the effects of different microwave power levels and application times. It is well-known that the level of the microwave power applied affects the generation of heat, and that even at high levels of microwave power the duration of the application must also be sufficient to effect curing.

Fig. 4.36 shows the temperature inside the microwave-cured reinforced paste samples and their power history in regard to the applying microwave energy at 50 watt for 30 minutes, 150 watt for 15 minutes, and 50 watt for 90 minutes. It was also found that the rate at which the temperature increases is related to a decreasing water-to-cement mass ratio; that is, the sample with the low water-to-cement mass ratio increases its temperature more rapidly than do the other samples. For the same reason aforementioned, the sample with the lowest water-to-cement ratio has higher concentrations of Ca^{2+}, Si^{4+}, and so on, than do the samples with higher water-to-cement ratios.

When comparisons the rate of temperature rise at the early period on microwave curing, a higher microwave power can generate heat (temperature) inside the sample higher than that of the lower microwave power. It corresponds to high microwave power; that is high electric field intensity.

However, microwave energy applied for longer duration can induce a higher temperature rise than energy applied for a shorter duration. For example, microwave energy of 50 watt applied for 90 minutes shows a final temperature increase of 112 ^{0}C and microwave energy of 150 watt applied for 15 minutes shows a final temperature increase of 62 ^{0}C. This suggests that as the duration of microwave energy application increases so the heat accumulated by the microwave energy accumulates and is added to the heat produced by the hydration reaction. Further, microwave energy applied for a long enough period encompasses the initial and final setting times, which both accrue more heat hydration, the latter accruing the most, when compared to the dormant period.

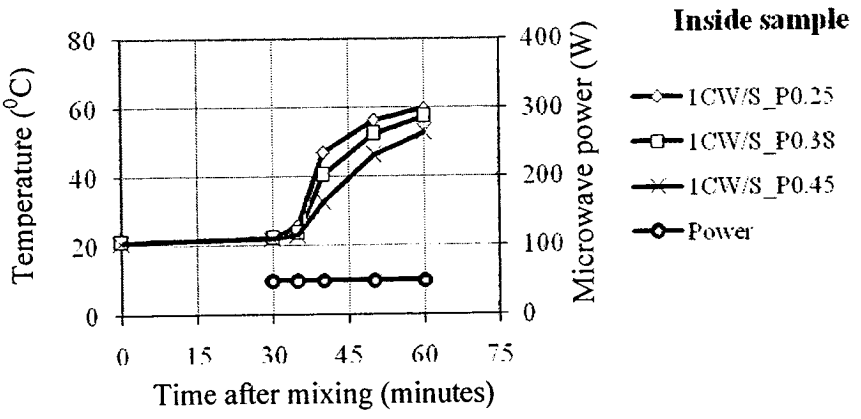

(a) Power level at 50 watt for 30 minutes

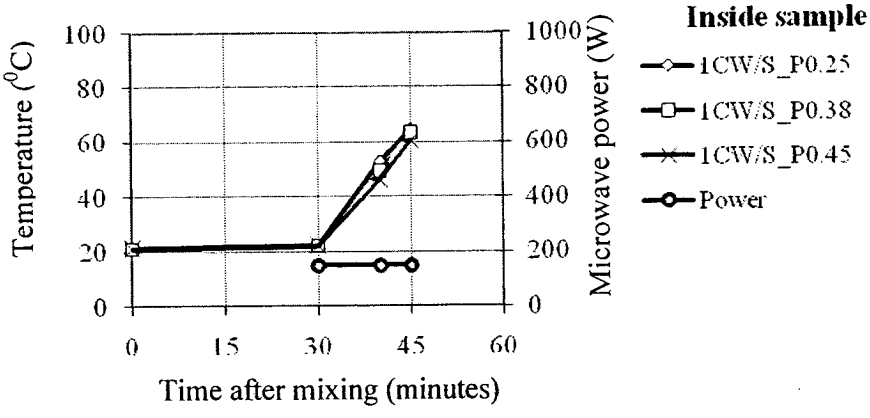

(b) Power level at 150 watt for 15 minutes

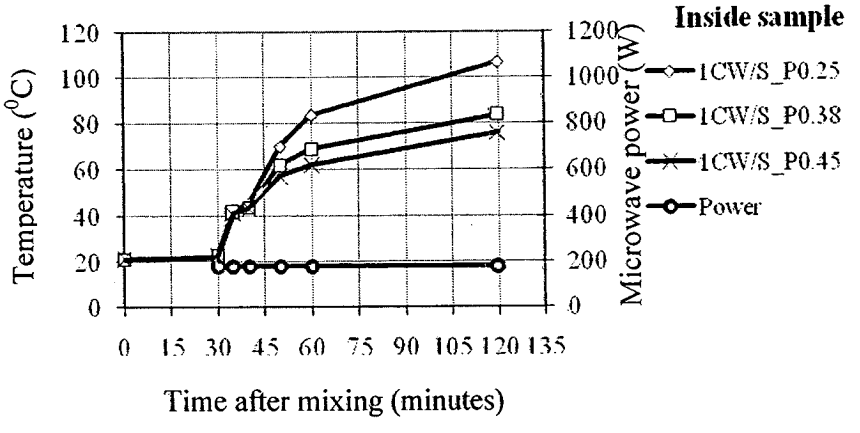

(c) Power level at 50 watt for 90 minutes

Fig. 4.36 Temperature and power history during applying microwave energy of various reinforced cement pastes with different power levels and times of application.

As shown in Fig. 4.37, a comparison of the morphology of the paste 1CW/S_P0.38 subjected to microwave curing of 100 watt for 30 minutes with that subjected to 150 watt for 15 minutes shows that overall they are similar in shape. However, the paste subjected to microwave power of 100 watt for 30 minutes shows a more plate-like shape than does the paste subjected to 150 watt for 15 minutes. It may be that a higher microwave power causes evaporation to take place immediately and then effects agglomeration in the paste sample. In other words, the rapid drying of the water present in the sample may cause the cement particles covered by the water molecules to bind together [135].

Fig. 4.38 shows the atom ratio of Si/Ca versus Al/Ca for the 1CW/S_P0.25, 1CW/S_P0.38, and 1CW/S_P0.45 pastes with different power levels and application times of microwave energy. In 0.25 w/s cement paste, an increase in the microwave power level does not affect the Si/Ca and Al/Ca ratios; however, an increase in the power level with a longer time of application decreases the Si/Ca and Al/Ca ratios. It can clearly be seen that both Si and Al elements are sensitive to electromagnetic waves. And, the same 0.38 w/s cement paste manifests the same behavior as does the 0.25 w/s cement paste. Nevertheless, the 0.45-w/s cement paste exhibits the opposite feature; that is, a longer application times increases the Si/Ca and Al/Ca ratios. This means that the presence of a comparatively large quantity of water, especially capillary water, in the cement-paste system affects the formation and configuration of the paste's products (C–S–H).

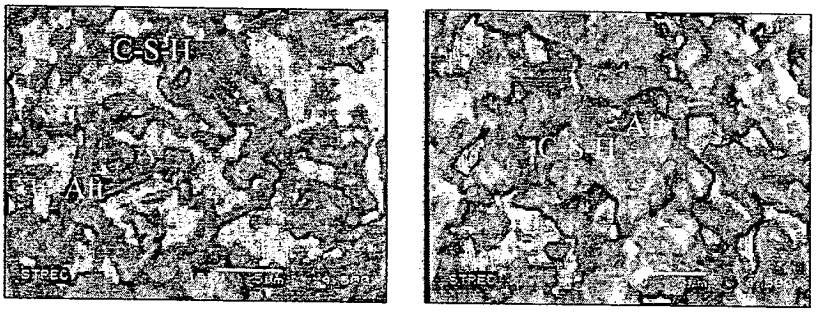

(a) 1CW/S_P0.38 after applying microwave energy power 100 watt for 30 minutes

(b) 1CW/S_P0.38 after applying microwave energy power 150 watt for 15 minutes

Fig. 4.37 Micrographs of 1CW/S_P0.38 reinforced cement pastes with different power levels and application times of microwave energy.

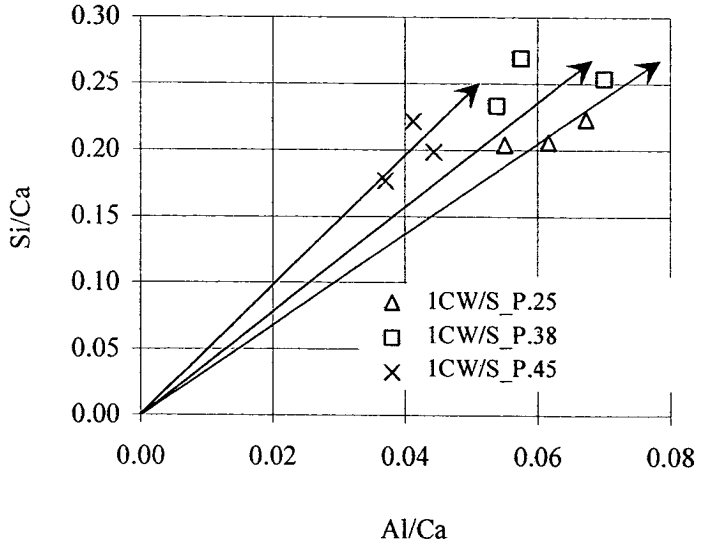

(a) Microwave power 50 watt for 30 minutes

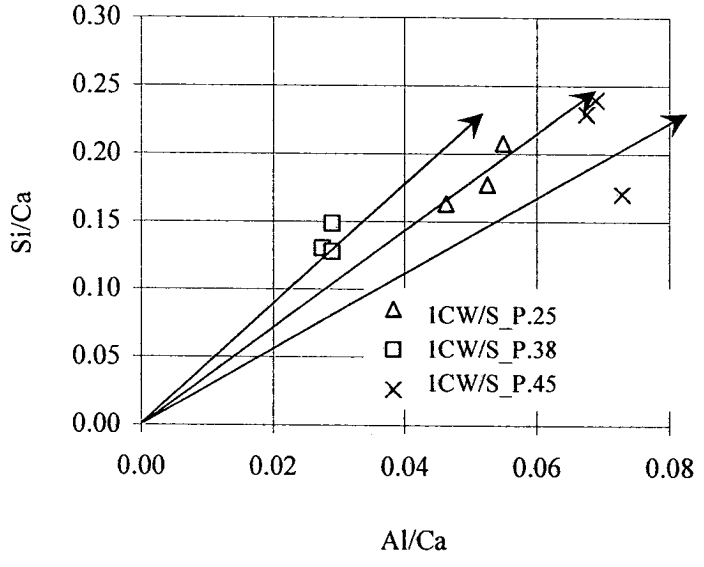

(b) Microwave power 50 watt for 90 minutes

Fig. 4.38 Atom ratio of Si/Ca versus Al/Ca of the pastes of 1CW/S_P0.25, 1CW/S_P0.38 and 1CW/S_P0.45 with different power levels and application times of microwave energy.

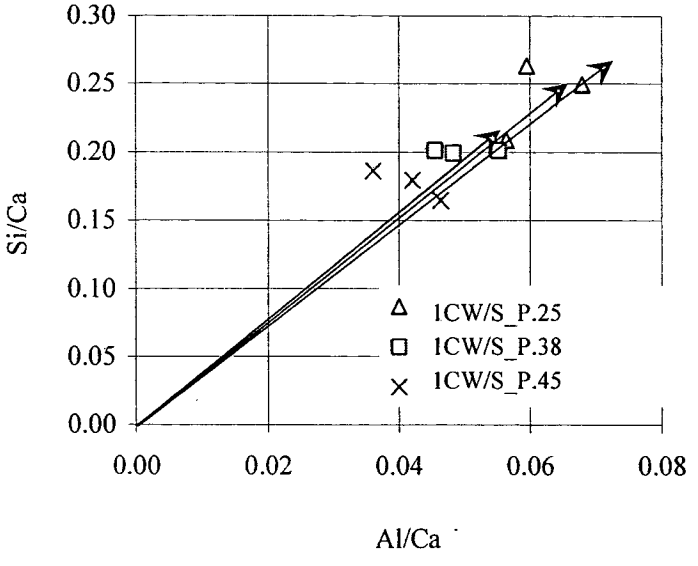

(c) Microwave power 150 watt for 15 minutes

Fig. 4.38 (Cont.) Atom ratio of Si/Ca versus Al/Ca of the pastes of 1CW/S_P0.25, 1CW/S_P0.38 and 1CW/S_P0.45 with different power levels and application times of microwave energy.

The effect of different power levels and application times of microwave energy on the phase characteristics of 1CW/S_P0.38 is shown in Fig. 4.39. It is found that the calcium silicate hydrate (Ca_3SiO_5), calcium hydroxide ($Ca(OH)_2$) lime (CaO) and Xenotile phases are similar.

The compressive strengths of 1CW/S_P0.25, 1CW/S_P0.38, and 1CW/S_P0.45 with a power level of 173 watt for 45 minutes, 173 watt for 90 minutes, and 782 watt for 15 minutes are shown in Fig. 5.48. The pastes show similar behavior in regard to compressive strength development; that is, compressive strength develops most quickly in the first 28 days.

The different power levels and application times of microwave energy affect the compressive strength of the microwave-cured pastes. A higher microwave power level causes C–S–H to take on an irregular shape, and it also causes thermal cracking (Haddad and Al-Qadi, 1998). It can be seen that at 28-days, the compressive strength of the 0.25 w/s microwave-cured paste shows a lower value than do the other samples. However, when the water-to-cement ratio of the paste increases, this effect is lessened.

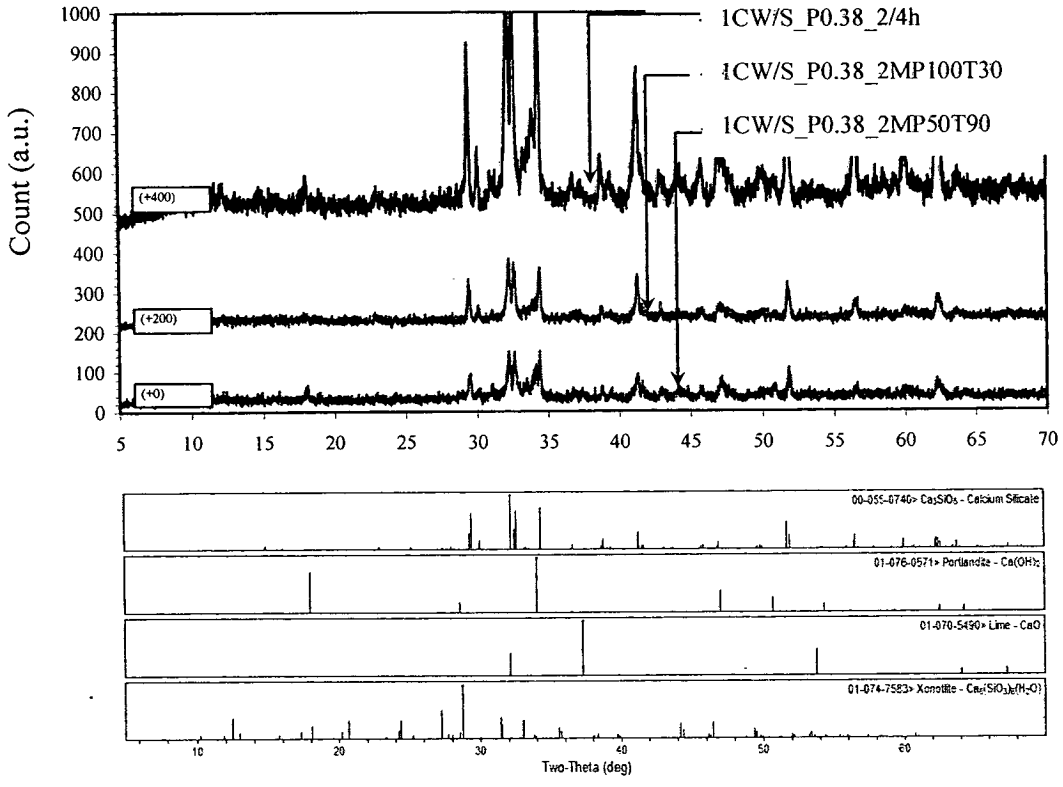

Fig. 4.39 X-ray diffraction the pastes of 1CW/S_P0.38 with different power levels and application times of microwave energy.

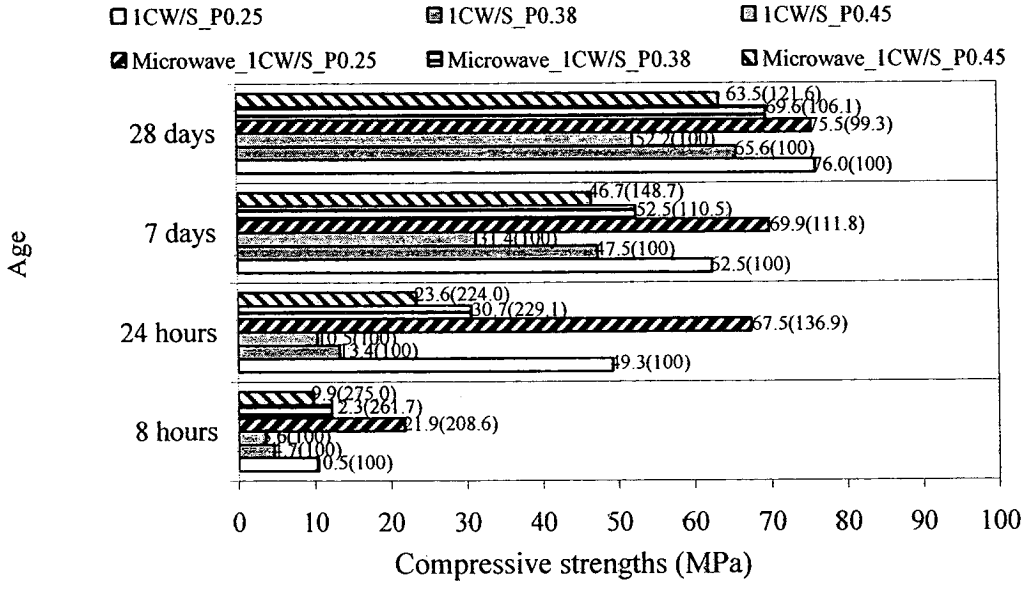

(a) Reinforced pastes when subjected to a power level 50 watt for 30 min.

Fig. 4.40 Compressive strengths the reinforced pastes of 1CW/S_P0.25, 1CW/S_P0.38 and 1CW/S_P0.45 with different power levels and application times of microwave energy.

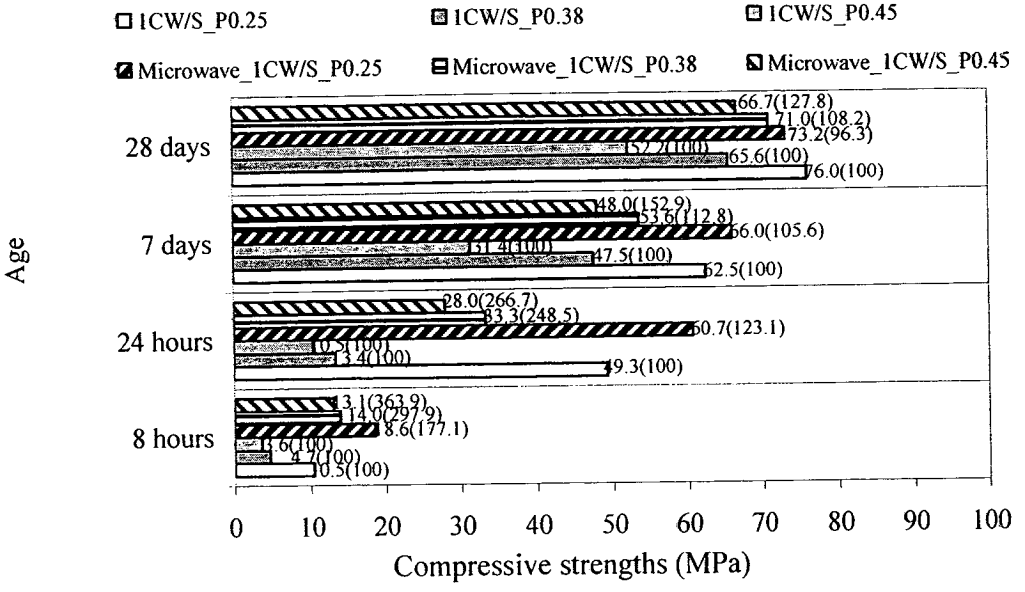

(b) Reinforced pastes when subjected to a power level 50 watt for 90 min.

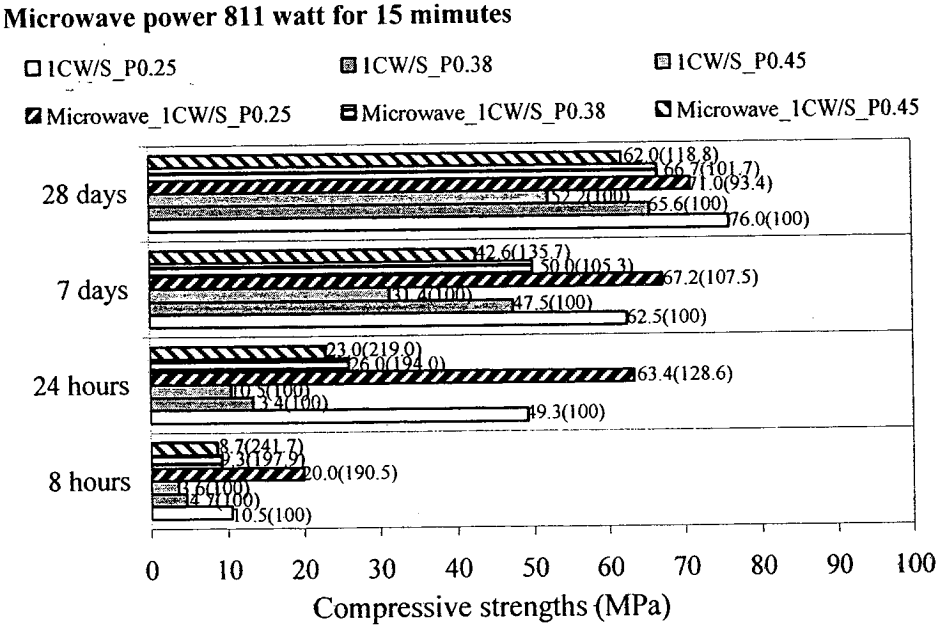

(c) Reinforced pastes when subjected to a power level 150 watt for 15 minutes.

Fig. 4.40 (Cont.) Compressive strengths the reinforced pastes of 1CW/S_P0.25, 1CW/S_P0.38 and 1CW/S_P0.45 with different power levels and application times of microwave energy.

4.5 Concluding remarks

Microwave energy can accelerate hydration reaction or increase the temperature within the microwave-cured reinforced cement sample; the effects of water-to-solid mass ratios, pozzolan materials, reinforced mortar and concrete, delay times, power level, and application duration were taken into account. The test results showed that the temperature increases monotonically among the positions of measurement during the microwave-curing process. The typical micrographs of the microwave-cured reinforced paste at the age of 4 hours after mixing, 28 days after curing in lime-saturated deionized water, and when subjected to microwave energy showed that the samples consisted of hydrated phases and pores, as well as cores of $Ca(OH)_2$ dendrite crystals or other crystals (marked CH), C–S–H, and granular structure. Furthermore, some ettringite (Aft) was found in the samples cured by microwave energy. From the SEM–EDS results it was observed that although the measured Ca/Si ratios of the pastes were similar in magnitude, they consistently decreased when the temperature decreased. For compressive strengths, the microwave-cured reinforced pastes developed strength quite rapidly, which correspond to the maintenance of the microwave power and time of application, and the water content of the pastes' hydration products were affected depending on the w/s; in addition, the $Ca(OH)_2$ contents were affected due to the completion of hydration reaction.